JGR Biogeosciences

RESEARCH ARTICLE
10.1029/2020JG005744

Key Points:

- Marsh dissolved organic matter export showed strong seasonal dependence, but seasonal variability in its quality was significantly lower
- Exposure to light increased the bioavailability of marsh-exported chromophoric dissolved organic matter (CDOM)
- Photobleaching decreased humic-like CDOM fluorescence, but increased microbial production of humic-like CDOM fluorescence

Supporting Information:

- Supporting Information S1

Correspondence to:
M. Tzortziou,
mtzortziou@ccny.cuny.edu

Citation:
Logozzo, L., Tzortziou, M., Neale, P., & Clark, B. J. (2021). Photochemical and microbial degradation of chromophoric dissolved organic matter exported from tidal marshes. *Journal of Geophysical Research: Biogeosciences*, *126*, e2020JG005744. https://doi.org/10.1029/2020JG005744

Received 7 APR 2020
Accepted 21 FEB 2021

Photochemical and Microbial Degradation of Chromophoric Dissolved Organic Matter Exported From Tidal Marshes

Laura Logozzo[1,4], Maria Tzortziou[1], Patrick Neale[2], and J. Blake Clark[3]

[1]Center for Discovery and Innovation, The City College of New York, The City University of New York, New York, NY, USA, [2]Smithsonian Environmental Research Center (SERC), Edgewater, MD, USA, [3]NASA Goddard Space Flight Center, NASA Postdoctoral Program, Greenbelt, MD, USA, [4]Now at School of the Environment, Yale University, New Haven, USA

Abstract Wetlands export chromophoric dissolved organic matter (CDOM) to estuaries, where CDOM is removed and transformed through biotic and abiotic process, subsequently impacting nutrient cycling, light availability, ecosystem metabolism, and phytoplankton activity. We examined the bioavailability and photoreactivity of CDOM exported from four Chesapeake Bay tidal marshes across three seasons and along an estuarine salinity gradient using three incubation treatments: 14-day microbial (MD), 7-day combined photochemical/microbial (PB + MD), and 7-day microbial incubation after photobleaching (MD after PB). CDOM absorption at 300 nm ($a_{CDOM}300$) and dissolved organic carbon (DOC) concentrations showed strong seasonality, with minima in winter, but CDOM quality (absorption spectral slopes, fluorescence component ratios) was less variable seasonally. PB + MD over 7 days decreased $a_{CDOM}300$ (−56.0%), humic-like fluorescence (−67.6%), and DOC (−17.8%), but increased the spectral slope ratio S_R (=$S_{275–295}$/$S_{300–350}$) (+94.8%), suggesting a decrease in CDOM molecular weight. Photochemistry dominated the PB + MD treatment. Photoreactivity was greater during the winter and in marsh/watershed versus down-estuary sites, likely due to less previous light exposure. Prior photobleaching increased the bioavailability of marsh-exported CDOM, resulting in a greater loss of $a_{CDOM}300$ and DOC, and a greater increase in humic-like fluorescence (−6.0%, −5.9%, and +18.4% change, respectively, over 7-day MD after PB incubations, vs. −2.8%, −5.5%, and +2.6% change, respectively, over 14-day MD incubations). CDOM exported from a marsh downstream of a major wastewater treatment plant showed the greatest photoreactivity and bioavailability. This highlights the significance of human activity on estuarine CDOM quality and biogeochemical cycles.

Plain Language Summary Marshes are sources of colored dissolved organic matter (CDOM) to estuaries, where CDOM can be transformed or removed by ultraviolet (UV) radiation or microbes. We examined CDOM susceptibility to UV radiation and microbial degradation from four Chesapeake Bay marshes and along a down-estuary salinity gradient, using incubation experiments with samples collected in the summer, fall, and winter. Our results showed that although more CDOM is exported by marshes in the summer, the quality of this material (based on optical proxies for CDOM composition) was consistent seasonally and interannually. Microbial processing removed a small, but significant, amount of CDOM and increased the contribution of humic-like CDOM typically associated with terrestrial sources. Microbial degradation combined with UV exposure decreased the amount of CDOM and the contribution of humic-like CDOM. Microbial degradation after exposure to UV light resulted in a greater loss of DOC and more production of humic-like CDOM compared to microbial degradation alone, suggesting exposure to light enhances the microbial utilization of marsh-exported CDOM. A marsh downstream of a major wastewater treatment plant exported CDOM that was more susceptible to UV and microbial degradation, suggesting that human activity can have significant effects on estuarine biogeochemical cycles, water quality, and ecosystem productivity.

1. Introduction

Dissolved organic matter (DOM) is one of the most important biogeochemical components influencing productivity, nutrient cycling, and optical properties of aquatic environments. DOM fuels heterotrophic

production in inland and coastal waters by providing carbon and nitrogen (Fellman et al., 2008), it limits the amount of UV-radiation and visible light in the ocean (Bricaud et al., 1981), and it makes up one of the largest reservoirs of carbon, with marine DOM storing as much carbon as that in atmospheric CO_2 (Hansell et al., 2009). DOM is the soluble portion of organic matter, operationally defined as organic molecules that pass through a 0.2 μm filter (Putter, 1907). It is primarily composed of dissolved organic carbon (DOC), in addition to dissolved organic nitrogen, dissolved organic phosphorous, and dissolved organic sulfur, thus contributing to the nutrient pool in aquatic environments. The optically active fraction of DOM that absorbs light selectively is known as chromophoric dissolved organic matter (CDOM) and a portion of the CDOM pool also fluoresces.

In coastal waters, CDOM is a complex mixture of allochthonous plant or soil derived compounds exported by rivers and wetlands and autochthonous sources derived from phytoplankton and detritus (Hedges, 1992; Maie et al., 2007; Qualls et al., 1991; Rochelle-Newall & Fisher, 2002; Tzortziou et al., 2008). Rivers and estuaries export 0.2 ± 0.05 Pg of DOC annually (Dai et al., 2012; Meybeck, 1982; Seitzinger et al., 2005), making these systems along the terrestrial-aquatic interface important sources of DOM to marine ecosystems. However, only a relatively small portion of terrigenous DOM makes up the oceanic DOM pool (Hedges, 1992), indicating rapid loss and transformation by flocculation and microbial and photochemical degradation processes in estuaries.

A particularly important source of terrestrial DOM to coastal ecosystems is tidal wetlands (T. Jordan et al., 1991; Jordan et al, 1983; Nixon, 1980; Tzortziou et al., 2011, 2008; Wetzel, 1992), which export large quantities of CDOM that is optically distinct from the surrounding aquatic system (Thurman, 1985; Tzortziou et al., 2008). As a result, wetland CDOM has numerous impacts on the biogeochemistry, optical properties, and biology of coastal waters, and often provides the carbon inputs necessary to sustain the net heterotrophy of estuarine ecosystems (Schlesinger & Bernhardt, 2013). Recent studies suggest that the lateral flux of total carbon from tidal wetlands to estuaries is 16 ± 10 Tg C per year for North America, but these estimates are characterized by particularly high uncertainty (Windham-Myers et al., 2018). Net export of dissolved carbon is poorly constrained by observations in these ecosystems, and, thus, wetland contributions of CDOM and DOC to adjacent waters are often not included in coastal ocean photochemical and biogeochemical models (Ward et al., 2020; Windham-Myers et al., 2018).

Wetland-exported CDOM tends to be mainly humic-like (i.e., made up of compounds such as lignin, tannins, and polyphenols with high molecular weight and high aromaticity), and therefore, more strongly light absorbing (C. D. Clark et al., 2008; Tzortziou et al., 2008; Wagner et al., 2015). While photochemical degradation of terrestrial CDOM has been shown to lead to an increase in its lability (Moran et al., 1999; Tranvik et al., 1999), its influence on the bioavailability of marsh-exported CDOM specifically has not been as widely studied. Recent studies acknowledge the contribution of labile CDOM from bogs and forested wetlands (Fellman et al., 2008), but the relative importance of environmental factors and source material is largely unknown. The photoreactivity and bioavailability (two factors that make up CDOM quality) of marsh-exported CDOM and how these vary seasonally, inter-annually, and across marsh systems is not well-characterized. This limits representation of these key processes in ecosystem models and increases uncertainty in predictions of the fate of this carbon pool in the coastal ocean. As a result, an essential piece in understanding the dynamics and functioning of temperate estuaries is missing, making it difficult to predict the impacts of climate and coastal land-use changes on coastal biogeochemical cycling and estuarine productivity.

We conducted a series of incubation experiments to characterize the quantity and quality of DOM exported from four tidal marsh systems in the Chesapeake Bay and associated tidal rivers, characterized by different vegetation properties, water quality, and salinity regimes. The bioavailability and photoreactivity was measured for DOM exported from these marsh systems (GCReW, Jug Bay, Taskinas, and Sweet Hall) and along a salinity gradient in the Rhode River sub-estuary. For each set of incubations, the influence of photochemical transformations on the bioavailability of DOM was also assessed. Incubations were performed under the same experimental conditions (i.e., temperature, light exposure) for DOM samples collected in the summer, fall, and winter to characterize seasonal and source-related differences in DOM microbial and photochemical degradability. Measurements across freshwater, brackish and heavily human-influenced marsh systems provide new insights into the role of marsh DOM outwelling in estuarine photochemical

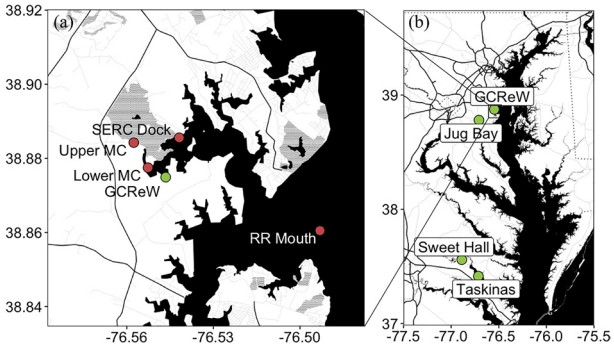

Figure 1. (a) Sampling sites on the Rhode River sub-estuary, and (b) marsh sampling sites on Chesapeake Bay. Marsh sites are denoted in green. Map tiles by Stamen Design, under CC BY 3.0. Data by OpenStreetMap, under ODbL. Plotted using ggmap (Kahle & Wickham, 2013).

processes, biogeochemical cycles, and microbial ecology. The marshes and sub-estuary analyzed in this study have characteristics typical of temperate marshes and sub-estuaries, and as such, may be representative of many coastal systems in other temperate regions.

2. Methods

2.1. Research Sites

To quantify the lability and photoreactivity of estuarine and marsh-exported DOM across different systems and seasons, incubation experiments were performed on samples collected from tidal creeks draining freshwater and brackish marshes in Chesapeake Bay over the summer and fall of 2016, the winter of 2016–2017, and along a salinity gradient on the Rhode River sub-estuary in the summer of 2016 (Figure 1; Table 1). The Kirkpatrick Marsh, also known as the Global Change Research Wetland (GCReW), is a high-elevation, brackish tidal marsh located on the Rhode River sub-estuary and is the main wetland source of DOM to the Rhode River (J. B. Clark et al., 2020; Jordan et al., 1983; Tzortziou et al., 2011, 2008). It is located near the Smithsonian Environmental Research Center (SERC) and is dominated by *Spartina patens, Spartina cynosuroides, Distichlis spicata, Iva frutescens,* and *Scirpus olneyi* (Jordan et al., 1983). Taskinas is a brackish tidal marsh located on the York River and is dominated by *Spartina patens* and *Distichlis spicata* (Perry & Atkinson, 1997). Jug Bay and Sweet Hall are freshwater marshes. Jug Bay is located on the Patuxent River and is highly influenced by urban and suburban development (Swarth et al., 2013); it is also located directly down-stream (<4 km) of a major wastewater treatment plant (WWTP), with a capacity of 30 million gallons per day, that has been reported to contribute 29% of the N-load and 48% of the *P* load of all WWTPs to the Patuxent River (Karrh et al., 2013). While the WWTP began implementing enhanced nutrient removal (ENR) techniques in 2011 and nutrient concentrations in the river decreased, phosphates remained relatively high, particularly in the summer and fall, indicating that the WWTP continues to contribute to nutrient concentrations despite ENR implementation. The Jug Bay system has a mix of persistent and primarily

Table 1
Dates and Sampling Sites for Incubation Experiments Performed From June 2016 to January 2017

Incubation ID	Sampling site(s)	Latitude/Longitude	Date of sampling	Incubation start
16-6	Upper MC	38.8843, −76.5576	6/28/2016	6/28/2016
	RR Mouth	38.8605, −76.4931	6/28/2016	
16-6	Lower MC	38.8775, −76.5527	6/29 /2016	6/29/2016
16-7	Jug Bay	38.7807, −76.7081	7/20/2016	7/20/2016
	Taskinas	37.4150, −76.7144	7/18/2016	
16-7	GCReW	38.8749, −76.5465	7/21/2016	7/21/2016
	SERC Dock	38.8856, −76.5419	7/21/2016	
16-8	GCReW	38.8749, −76.5465	10/19/2016	10/20/2016
	Sweet Hall	37.5589, −76.8883	10/18/2016	
16-8	Taskinas	37.4150, −76.7144	10/18/2016	10/21/2016
	Jug Bay	38.7807, −76.7081	10/19/2016	
17-1	GCReW	38.8749, −76.5465	1/5/2017	1/7/2017
	Jug Bay	38.7807, −76.7081	1/5/2017	
17-1	Taskinas	37.4150, −76.7144	1/5/2017	1/8/2017
	Sweet Hall	37.5589, −76.8883	1/5/2017	

GCReW, Global Change Research Wetland; Lower MC, Lower Muddy Creek; RR Mouth, Rhode River Mouth; SERC, Smithsonian Environmental Research Center; Upper MC, Upper Muddy Creek.

non-persistent emergent vegetation, including *Leersia oryzoides, Hibiscus moscheutos, Peltandra virginica, Phragmites australis, Polygonum arifolium,* and *Typha* × *glauca* (high marsh) and *Nuphar lutea, Pontederia cordata,* and *Zizania aquatica* (low marsh) (Swarth et al., 2013). Sampling was conducted near the low marsh portion of Jug Bay, making the vegetation characteristics at the sampling site distinct from the other marshes. Sweet Hall is located on the York River and is dominated by *Peltandra virginica, Carex stricta, Leersia oryzoides, Polygonum punctatum,* and *Polygonum arifolium* (Perry & Atkinson, 1997).

In addition to sampling at GCReW, we also sampled a number of sites along a down-estuary salinity gradient along the Rhode River at low tide: Upper Muddy Creek (Upper MC), Lower Muddy Creek (Lower MC), the SERC Dock and the Rhode River Mouth (RR Mouth) (Figure 1; Table 1). Upper Muddy Creek is located in an upstream reach of Muddy Creek (the main source of freshwater to the Rhode River), and is surrounded mostly by forest and mud flats, and thus CDOM from this site can be considered "non-marsh terrestrial" or watershed CDOM (Tzortziou et al., 2011). Lower Muddy Creek is located at the intersection of Muddy Creek and the Rhode River, and therefore, waters there receive a mixture of watershed and "estuarine" CDOM. The influence of GCReW may also be significant at Lower Muddy Creek. Water at the SERC Dock contains a mixture of marsh and estuarine CDOM, but with less marsh influence than waters closer to GCReW (Tzortziou et al., 2011). Lastly, the Rhode River Mouth is where the confluence of the Rhode and West Rivers opens to the main stem of Chesapeake Bay; it is therefore the most down-estuary endmember of all the sites (Tzortziou et al., 2011, 2008). Tzortziou et al. (2011) showed that along a gradient from GCReW to the Rhode River mouth at low tide, mixing was nonconservative for DOC and CDOM absorption and fluorescence, suggestive of DOC and CDOM degradation and/or transformation by photochemistry in particular (J. B. Clark et al., 2020). Therefore, sites along this gradient at low tide are representative of differences in DOC and CDOM quality both due to dilution with estuarine water and prior photochemical transformation during transport.

2.2. Sample Collection and Filtering

Water samples were collected at each site within a time-window of ±30 min from low tide, stored in the dark at 4°C, and in almost all cases filtered immediately upon collection (<1 day storage) for 2-week dark and light incubation experiments. For marsh-exported CDOM, water samples were collected at tidal creeks draining each marsh ±30 min from low tide, when the influence of marsh outwelling on adjacent estuarine water properties is the strongest (C. D. Clark et al., 2008; Jordan et al., 1983; Tzortziou et al., 2008).

We used glass-fiber filters (GF/F, nominal pore size of 0.7 μm) to remove particulate material, but to retain some bacteria in the filtrate. It is important to note that only a portion (35%–43%, according to Lee et al., 1995) of the total bacterial cell count passes through a GF/F and that the filter preferentially removes larger cells (i.e., diameters greater than 0.7 μm). 100 mL of the filtrate was distributed either into combusted 120 mL amber bottles (dark treatments) or acid-soaked Teflon (Nalgene FEP) bottles (light treatments) (Text S1, Figure S1).

A portion of the GF/F filtrate was also subsequently filtered through a 0.2 μm filter (Nuclepore) and kept in the dark for 14 days as a presumed "control" treatment, or exposed to 7 days of light as presumed "photobleaching-only" treatment. Although most studies have assumed samples filtered through a 0.2 μm filter contain no bacteria (Lu et al., 2013; Stedmon & Markager, 2005; Zhang et al., 2013), we report here data on microbial cell counts showing that in our systems, enough inoculum passes through 0.2 μm filters to result in significant microbial growth in these fractions (see Results). Similar results were previously reported across a variety of ecosystems (Brailsford et al., 2017; Elhadidy et al., 2016; Liu et al., 2019; Obayashi & Suzuki, 2019; Wang et al., 2008). Other results from these treatments (e.g., photoreactivity estimates) are not presented since the presence of bacteria confounds their interpretation as "control" or "photobleaching-only."

2.3. Incubations

There were three treatments for the incubations: 14-day dark incubation (to assess microbial-only degradation, "MD"), 7-day light incubation (combined photochemical and microbial degradation "PB + MD"), and a 7-day dark incubation following the 7-day light incubation (to examine effects of previous light exposure

on microbial degradation, "MD after PB"). The lengths of the incubations were chosen based on a typical residence time of a conservative tracer in the Rhode River from head of tide to the mouth of the sub-estuary, which is about 7 days under low flow conditions (T. E. Jordan et al., 1991). All three treatments were incubated at 24°C (details in Text S2), in order to remove temperature as a potential confounding variable impacting DOM bioavailability and photoreactivity. The incubation temperature was chosen as 24°C since this is close to the average summer surface water temperature on the Rhode River. Incubations were started within 1–2 days of sample filtration; treatments were kept in the dark at 4°C until the start of the incubations. Four replicate bottles were used for the microbial-only treatment (14-day incubation) and three each for the combined photochemical and microbial (7-day incubation) and microbial after photobleaching (7-day incubation) treatments; only three replicate bottles were used for the light incubations due to space limitations in the UV-exposure set-up. The microbial-only treatment remained in the dark over the course of the 14-day incubation and the bottles were inverted once per day to reduce settling and aggregation. For the combined photochemical and microbial treatment, a UV-transmitting acrylic Plexiglas sheet was placed approximately one inch above two Q-labs UVA340 lamps. The Teflon bottles with 100 mL of the sample filtrate were placed on top of the UV-transmitting acrylic sheet ("Plexiglas"), in two rows above the lamps with the bottles centered on each lamp tube (Figures S2 and S3). The 100 mL of filtrate filled the Teflon bottles to a depth of about 4 cm. These bottles were also inverted once per day to reduce settling, and their positions above the lamp were displaced each day so that all bottles received approximately the same exposure over the course of the incubation.

UV spectral irradiance (284–650 nm) was measured at the upper surface of the Plexiglas at each bottle position using a fiber optic spectroradiometer as described by Neale and Fritz (2002). While UVA340 lamps mainly emit in the UV (Figure S4), there is also a minor emission in the PAR (400–700 nm) mostly from emission lines at 436 and 546 nm. Scalar (4π) measurements of this PAR emission (on the order of 10 μmol m^{-2} s^{-1}) were made at each bottle position both at the upper surface of the Plexiglas (dry) and at mid-depth in the incubation bottles with 100 mL of deionized water using a QSL 2100 probe (Biospherical Instruments). The in-bottle/upper-surface ratio of PAR together with the spectral transmission of the Teflon bottles (relative to PAR, Figure S1) was applied to the upper-surface-measured UV spectrum to estimate within-bottle UV exposure. This adjustment accounted for the optical effects of refraction, scattering and spectral filtering by Teflon on within-bottle exposure. Average exposure to total UV irradiance (after accounting for filtrate self-shading, see Text S3) was 15.16 W m^{-2} (Table S1); absorbed UV exposure over 24 h was about the same as the UV-exposure over a cloud-free summer day (June 21) in the Rhode River surface water, based on the average CDOM absorption spectrum of each sample (see Text S3, Table S1 and Figure S4). While small phototrophic picoplankton may be present in GF/F filtrate, there was no evidence of any photosynthetic pigment absorbance in the spectral scans. For the effects of photobleaching on microbial ("MD after PB") treatment, GF/F-filtered water samples that were exposed to light for 1 week were placed in the dark for the second week to quantify the impacts of CDOM photochemical degradation on its microbial availability.

2.4. Microbial Cell Counts

At selected time points in the incubations of October 2016 and January 2017, a 1.8 mL aliquot was taken from each replicate incubation container (dark and light), fixed with 180 μL of 20% paraformaldehyde, flash frozen at −80°C, and stored until processed (within a week). For analysis, the samples were thawed and then stained with SYBR Green nucleic acid stain, incubating for at least 30 min. Cell count based on SYBR green fluorescence was performed with a BD C6 Accuri flow cytometer at the University of Maryland Center for Environmental Horn Point Laboratory Cell Analysis Center. Before each sample processing, the flow cytometer was validated with factory supplied 6- and 8- fluorescence peak beads according to the BD Accuri software guide standards (https://www.bdbiosciences.com/documents/BD_Accuri_CSampler_Software_User_Guide.pdf).

2.5. Measurements and Parallel Factor Modeling

Measurements were taken at three time points during the incubation: day 0, day 7, and day 14 (Text S4). Samples were stored in a refrigerator at 4°C until measurement, which occurred within two days of the incubation time point. The exception was October 2016, when travel to and from SERC prevented immediate

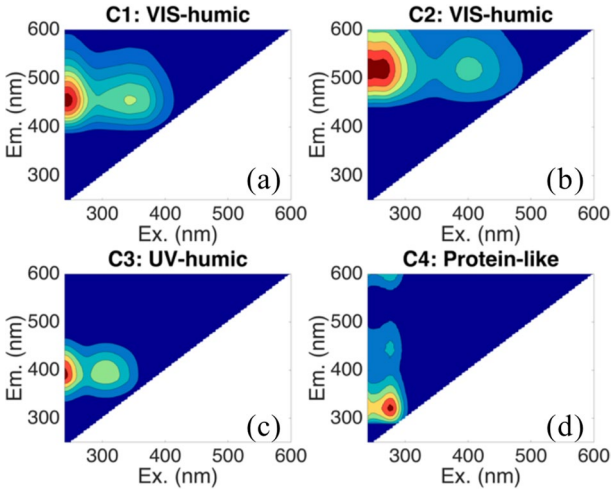

Figure 2. Four fluorescence components identified by our PARAFAC model. Components were identified as (a) shorter-wavelength visible-emitting humic-like (VIS-humic), (b) longer-wavelength VIS-humic, (c) UV-emitting humic-like (UV-humic), and (d) protein-like.

measurement; absorption and fluorescence measurements for this incubation were conducted within 2 weeks of the incubation time point. DOC concentrations were measured within three months of the incubation time point. All samples were stored in a refrigerator at 4°C between the incubation time point and the time of measurement; DOC samples were not acidified prior to analysis.

DOC concentrations were measured on a Shimadzu TOC-V CSH Total Organic Carbon analyzer using high temperature combustion. Determinations followed the manufacturer's recommended protocol for non-purgeable organic carbon based on calibration with potassium hydrogen phthalate.

CDOM absorption spectra ($a_{CDOM}[\lambda]$) were measured using a CARY-IV dual-beam spectrophotometer and 1 cm path-length, acid-washed and deionized water (DI)-rinsed, quartz cuvettes. Measurements (270–750 nm spectral range and at 2-nm resolution) were baseline corrected using DI, with a blank run at the beginning and end of the run, and every five samples. Duplicate measurements were performed on each sample. $a_{CDOM}(\lambda)$ was calculated from the optical density (OD) and path length (l_g, which for our measurements was 1 cm = 0.01 m):

$$a_{CDOM}(\lambda) = 2.303\frac{OD(\lambda)}{l_g}.$$

Consistent with other studies (C. D. Clark et al., 2008; Helms et al., 2008; Osburn & Stedmon, 2011), changes in CDOM absorption magnitude are reported at 300 nm ($a_{CDOM}300$). To examine changes in CDOM absorption spectral characteristics, we estimated the CDOM absorption slopes in the 275–295 nm spectral region ($S_{275–295}$) and the 350–400 nm spectral region ($S_{350–400}$) following Helms et al. (2008), by fitting a linear regression to the log-transformed $a_{CDOM}(\lambda)$ for each wavelength range (275–295 nm and 350–400 nm). Changes in the slope ratio S_R, defined as $S_R = S_{275–295}/S_{350–400}$, are also shown, as S_R was previously reported to be a good indicator of DOM molecular weight (MW) and photochemically induced shifts in MW across water types (Helms et al., 2008).

Fluorescence excitation-emission matrices (EEMs) were measured using a SPEX Fluoromax-3 spectrofluorometer. EEMs were measured for excitation wavelengths 240–600 nm (5 nm resolution) at emission wavelengths 250–600 nm (2 nm resolution). Fluorescence was corrected for absorption within the sample (inner-filter effect) using the absorption spectra measured spectrophotometrically following Kothawala et al. (2013). A DI EEM was measured for each set of sample EEMs run; after the inner-filter corrections, the DI EEM was subtracted from the sample EEM and then converted to Raman Units, using the area under the Raman scattering peak (excitation: 250 nm and emission: 370–428 nm).

EEMs were analyzed using parallel factor analysis (PARAFAC), a multivariate modeling technique that decomposes the CDOM fluorescence signature into individual fluorescence components (Stedmon & Bro, 2008). We compared the four PARAFAC components output from our model (Figure 2) to the OpenFluor database (Murphy et al., 2014). Descriptions of each component and references to similar components are described in detail in Table 2. The C1 fluorescence component (VIS-humic-like) was similar to terrestrial humic-like components from OpenFluor, and has been shown to be well-correlated with dissolved lignin concentration (Osburn, Boyd, et al., 2016). C2 (VIS-humic-like) was similar to spectra from soil fulvic acids and spectra from soil leachate (Osburn, Handsel, et al., 2016), and thus is described as terrestrial humic-like or soil fulvic-like fluorescence. C3 (UV-humic-like or marine-humic-like), is generally ubiquitous, and commonly present in estuarine and marine water, but also wastewater. It is often thought of as microbially produced (Coble, 1996). C4 was similar to the fluorescence spectra of aromatic amino-acids (Bianchi et al., 2014; Osburn, Boyd, et al., 2016), and thus is described as protein-like.

The percent change for each parameter over each incubation was estimated as the difference between the measurement at the end of the incubation (either day 7 or day 14) and initial (day 0) values, divided by the

Table 2
PARAFAC Components Identified in this Study and their Probable Sources

Component number	Component name	Excitation maximum (nm)	Emission maximum (nm)	Description	OpenFluor references
C1	VIS-humic-like	245 (350)[a]	456	Terrestrial humic-like	45 matches
					C1 (Osburn, Boyd, et al., 2016)
C2	VIS-humic-like	245 (400)	514	Terrestrial humic-like	35 matches
				Soil fulvic-like	C5 (Yamashita et al., 2010)
					C1 (Osburn et al., 2012)
					C4 (Osburn, Handsel, et al., 2016)
C3	UV-humic-like (marine humic-like)	< 240 (310)	392	Microbial humic-like	41 matches
				Ubiquitous, but commonly found in wastewater, estuarine, and marine water	C2 (Osburn, Boyd, et al., 2016)
					C2 (Murphy et al., 2011)
C4	Protein-like	275	322	Aromatic amino acid-like (Bianchi et al., 2014; Osburn, Boyd, et al., 2016)	4 matches
					C4 (Osburn, Boyd, et al., 2016)
					C4 (Bianchi et al., 2014)

PARAFAC, parallel factor analysis.
[a]Wavelength in parentheses is a secondary peak in excitation spectrum.

initial value and multiplied by 100%. The impacts of light exposure on microbial availability were determined by comparing the day 14 measurements to the day 7 measurements, where day 7 is the "initial" (i.e., the starting point for microbial degradation after 7 days of light exposure).

2.6. Statistical Analyses

We used one sample student *t*-tests to evaluate bioavailability and photoreactivity significance. We used two-way ANOVA combined with Tukey's pairwise differences test to evaluate the initial spectroscopic differences and differences in bioavailability and photoreactivity between sites and seasons. For comparison across the Rhode River sites only, we used one-way ANOVA with Tukey's pairwise differences test to evaluate significance. Statements of marginal means are accompanied by the residual standard error (RSE) used in the Tukey test.

3. Results

3.1. Initial Conditions

In the Rhode River sub-estuary, DOC concentrations decreased downstream from the marsh, from 650 μM at GCReW to 312 μM at the SERC Dock (Table 3). CDOM absorption ($a_{CDOM}300$) decreased down-estuary by a factor of 6, from 36.7 at GCReW to 6.23 m^{-1} at the Rhode River Mouth. S_R increased down-estuary, due to both the increase in $S_{275–295}$ and the decrease in $S_{350–400}$ with distance from terrestrial sites. CDOM fluorescence also decreased, particularly the VIS-humic-like components (C1 and C2). Both C1 and C2 were highest at GCReW (the marsh end-member) and they both decreased, proportionally, down-estuary with distance from terrestrial DOM sources. As a result, there was no spatial trend in the C2/C1 ratio (Table 3). The marine-humic-like (C3) and protein-like (C4) components also decreased down-estuary but to a lesser degree relative to C1 and C2, resulting in an increase in the C3/C1 and C4/C1 ratios down-estuary from 0.72 to 1.1 and from 0.14 to 0.54, respectively (Table 3).

Table 3
Parameters Initially (at Day 0) for Each Site and Incubation

Site	Incubation	DOC (μM)[a]	$a_{CDOM}300$ (m^{-1})	S_R	$S_{275–295}$ (nm^{-1})	$S_{350–400}$ (nm^{-1})	C1 (RU)	C2/C1	C3/C1	C4/C1
Upper MC	16-6/Jun 2016	N/A	20.5	1.03	−0.0186	−0.0179	1.12	0.32	0.72	0.14
Lower MC	16-6/Jun 2016	N/A	11.9	1.09	−0.0190	−0.0175	0.55	0.34	0.85	0.24
SERC Dock	16-7/Jul 2016	312 (4)	7.70	1.27	−0.0212	−0.0167	0.34	0.42	1.0	0.38
RR Mouth	16-6/Jun 2016	N/A	6.23	1.49	−0.0200	−0.0134	0.20	0.38	1.1	0.54
GCReW	16-7/Jul 2016	650 (15)	36.7	0.92	−0.0149	−0.0163	1.56	0.37	0.67	0.13
	16-8/Oct 2016	516 (3)	26.5	0.88	−0.0148	−0.0168	1.17	0.38	0.67	0.11
	17-1/Jan 2017	497 (9)	25.0	0.82	−0.0140	−0.0170	0.94	0.37	0.61	0.13
Jug Bay	16-7/Jul 2016	377 (10)	22.0	0.78	−0.0139	−0.0179	1.12	0.27	0.82	0.20
	16-8/Oct 2016	497 (11)	20.4	0.84	−0.0152	−0.0182	1.20	0.29	0.86	0.22
	17-1/Jan 2017	N/A	9.7	0.85	−0.0160	−0.0188	0.56	0.26	0.95	0.30
Sweet Hall	16-8/Oct 2016	610 (2)	41.6	0.79	−0.0135	−0.0167	1.60	0.33	0.61	0.10
	17-1/Jan 2017	403 (7)	20.3	0.84	−0.0143	−0.0170	0.84	0.32	0.70	0.16
Taskinas	16-7/Jul 2016	570 (2)	30.9	0.89	−0.0150	−0.0169	1.47	0.34	0.63	0.10
	16-8/Oct 2016	497 (5)	22.5	0.91	−0.0160	−0.0176	1.20	0.34	0.65	0.10
	17-1/Jan 2017	N/A	17.4	0.89	−0.0156	−0.0175	0.80	0.34	0.63	0.12

Note. Measurements performed on GF/F filtrate, equivalent to the 0.7 μm size fraction.

GCReW, Global Change Research Wetland; Lower MC, Lower Muddy Creek; SERC, Smithsonian Environmental Research Center; Upper MC, Upper Muddy Creek.

[a]Standard deviation for DOC measurements listed in parentheses.

Comparing CDOM properties across marshes, the largest CDOM absorption and fluorescence signals were measured at the freshwater Sweet Hall marsh system in October 2016 ($a_{CDOM}300 = 41.6\ m^{-1}$ and C1 = 1.60 RU) (Table 3). During the same month, $a_{CDOM}300$ and C1 varied only slightly across the other three marsh systems (in a narrow range of 20.4–26.5 m^{-1} and 1.17–1.20 RU, respectively). Dominated by non-persistent emergent marsh vegetation, and with the strongest anthropogenic influence, the Jug Bay system showed some unique marsh CDOM characteristics (Table 3). Lower $a_{CDOM}300$ and C1 fluorescence were measured in Jug Bay, particularly during the winter (9.7 m^{-1} and 0.56 RU, respectively), compared to the other marshes ($a_{CDOM}300$ and C1 in the range of 17.4–25 m^{-1} and 0.8–0.94 RU, respectively). Jug Bay also had a significantly steeper $S_{350–400}$ compared to GCReW and Sweet Hall ($P < 0.05$), and the highest ratios of the marine:humic (C3/C1) and protein:humic (C4/C1) fluorescence components ($P < 0.05$), particularly during the winter (Table 3).

The seasonal variation in CDOM absorption and fluorescence magnitude was pronounced and consistent across systems (Table 3). Both CDOM absorption ($a_{CDOM}300$) and CDOM fluorescence (particularly C1 and C3) decreased considerably from summer to winter for all the marsh sites ($P < 0.05$) and particularly for the freshwater marshes (i.e., Sweet Hall and Jug Bay) where $a_{CDOM}300$ decreased by more than a factor of two from October to January. Interestingly, compared to CDOM absorption and fluorescence magnitude, the CDOM absorption and fluorescence spectral shape (proxies for CDOM composition) showed considerably less seasonal variability. Specifically, the absorption spectral slopes S_R and $S_{275–295}$ and the fluorescence ratios C2/C1, C3/C1, and C4/C1 did not show any statistically significant differences seasonally ($P > 0.1$). Yet, initial values of $S_{350–400}$ for all marsh sites were statistically significantly steeper in the winter than the other months ($P < 0.05$) (see discussion in section §4.5).

3.2. Microbial Growth

Microbial cell count was sampled daily over 8 days for the dark incubations in October 2016, using 0.2 μm and GF/F filtrate from all four marsh sites. Although the initial bacterial counts in 0.2 μm filtrate were 1–2 orders of magnitude lower than the GF/F filtrate, bacterial growth in the 0.2 μm filtrates was rapid,

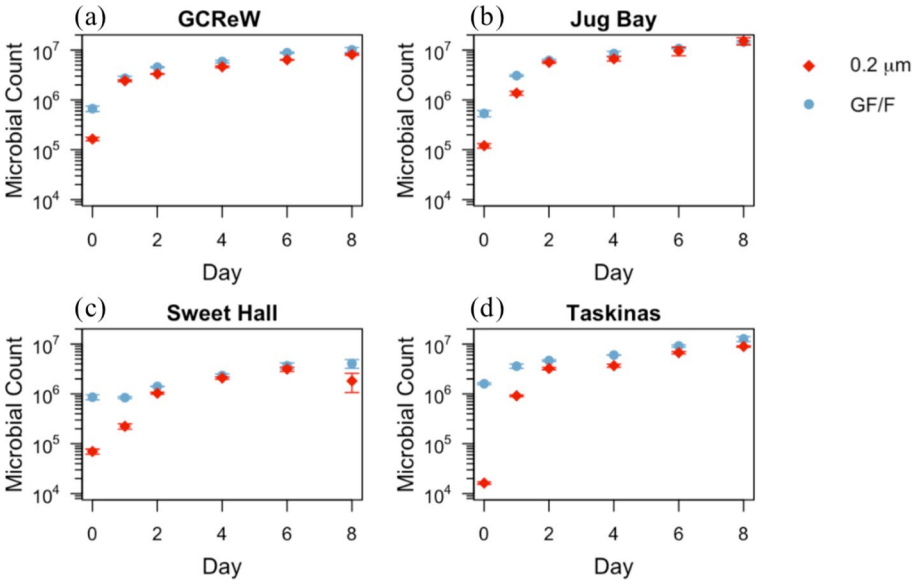

Figure 3. Microbial counts per mL for a microbial growth dark incubation test conducted in July 2016 for the four marsh sites. Error bars represent the standard deviation between three replicate measurements.

such that the cell count was close to that in the GF/F filtrate after 1–2 days and remained similar to the GF/F treatments thereafter for all four marsh sites (Figure 3). As a result, for the majority of the parameters analyzed here (e.g., $a_{CDOM}300$, S_R, $S_{275–295}$, $S_{350–400}$, C3 and C4) the 14-day "control" treatment showed changes that were very similar to and not significantly different than the 14-day microbial-only incubation ($P > 0.05$). The change in DOC was only significantly different ($P < 0.05$) between the two treatments at GCReW and Jug Bay.

In July 2016, microbial counts were made for both 0.2 μm and GF/F filtrates after the 7-day light incubation and 7-day dark incubation. Similar to the dark incubations from October 2016, the final counts in the 0.2 μm light filtrates were close to those in the GF/F filtrates, varying from 56% to 106% of the count in the GF/F filtrate (average 84%, standard deviation, SD = 25%) (Figure 4). Moreover, microbial counts in the 7-day light exposures of GF/F filtrates were the same or greater than the final counts after 7 days in the dark (mean Light/Dark 107%, SD = 10%). This shows that the modest UV irradiance in the light exposures did not significantly inhibit microbial growth. Similar results were obtained in a second set of counts made for incubations in January 2017 (data not shown). Given the influence of microbial activity in the 0.2 μm filtrates, the changes in DOC and optical properties during light exposure of these samples were not considered measures of photochemical degradation alone. Instead, we only present the combined PB + MD treatment (GF/F filtrate), and thus have no photobleaching-only treatment. While the observed microbial growth in the 0.2 μm filtrate did not allow to address the impact of photobleaching alone, the combined PB + MD treatment is more representative of natural conditions, since photochemical degradation and microbial degradation co-occur in the natural environment.

3.3. Microbial Degradation

DOC decreased for all marsh sites over the 14-day dark incubation by, on average, 5.5% (SD = 5.4%). Jug Bay had a significantly greater relative loss compared to the other three marsh sites (marginal means 11.7% vs. 2.7%–4.2% over 14 days, on average, RSE = 3.0%) ($P < 0.01$) (Figure 5a). The DOC loss was also significantly lower for samples collected in July 2016 than October 2016 and January 2017 ($P < 0.01$).

The absorption ($a_{CDOM}300$) of marsh exported CDOM consistently decreased over the 14-day incubation (Figure 5b), with Jug Bay showing significantly ($P < 0.05$) greater loss of $a_{CDOM}300$ compared to the other three marsh sites (marginal means 6.3% vs. 0.3%–2.4% over 14 days, RSE 2.9%) (Figure 5b). Overall, S_R increased during microbial degradation, with Jug Bay, again, showing a significantly higher increase in S_R

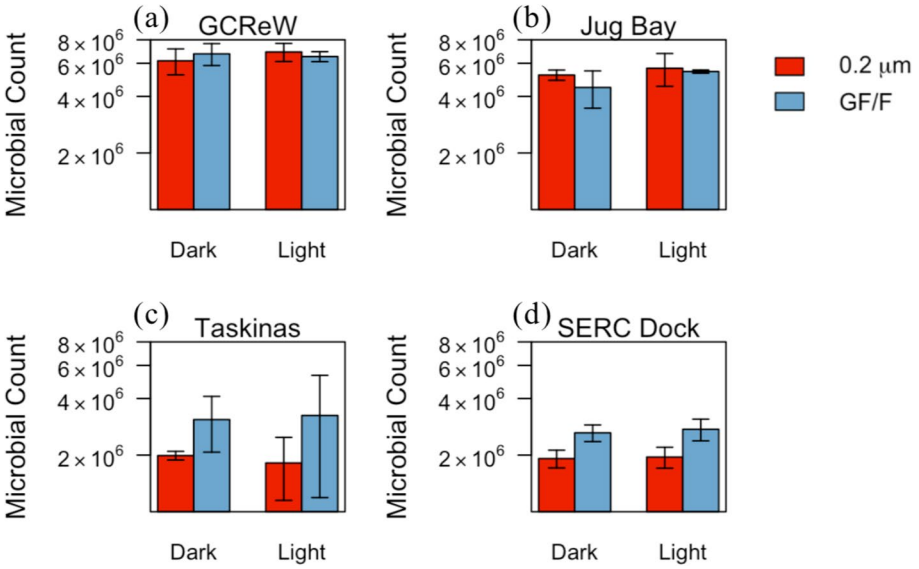

Figure 4. Microbial counts per mL for four sites in October 2016 after 7 days with or without light exposure for either 0.2 μm or GF/F filtrate. Error bars show the standard deviation for four replicate bottles (dark) and three replicate bottles (light).

compared to the other marshes (marginal means 8.7% vs. 2.2%–3.1% over 14 days, on average, RSE = 3.6%) ($P < 0.01$). In all cases, the increase in S_R was the result of a decrease in both $S_{275–295}$ and $S_{350–400}$, with a larger decrease in $S_{350–400}$ (Figures 5c–5e and 6a). Jug Bay also had a significantly higher loss in $S_{350–400}$ than the other marsh sites (marginal means 6.9% vs. 2.3%–4.2% over 14 days, on average, RSE = 2.3%) ($P < 0.05$). Microbial degradation had, overall, a smaller impact on the absorption of estuarine CDOM collected from the Rhode River, resulting in both an increase and a decrease in $a_{CDOM}300$ across the salinity gradient (Figure 6a).

For all sub-estuary and marsh sites, the humic-like fluorescence components (C1, C2, and C3) increased over the 14-day microbial incubation (with the exception of Jug Bay) (Figures 5f–5i and 6d). The average increase in C1 for all marsh sites was 2.5% after 14 days (SD = 2.4%) (Table 4), with the greatest increase occurring in January 2017. Across the Rhode River, C1 showed a larger increase at the mouth of the estuary compared to the GCReW marsh end-member ($P < 0.05$). Similar trends were observed for C2 and C3. Jug Bay was the only marsh system where the humic-like components decreased during the July and October 2016 incubations. Similarly, while the protein-like component (C4) showed a substantial increase for all the Rhode River sites (by 39.8% on average, SD = 47.1%) and most of the marsh sites, it consistently decreased at Jug Bay (Figures 6d and 5i).

3.4. Combined Photobleaching and Microbial Degradation

Microbial degradation coupled with photobleaching resulted in a decrease in DOC concentrations for all marsh sites by 17.8% on average (SD = 4.6%) over the 7-day light incubation (Table 4 and Figure 7a). Taskinas had a significantly lower overall DOC loss compared to Jug Bay and Sweet Hall ($P < 0.01$), though there were no significant differences seasonally.

Similar to microbial degradation alone, CDOM absorption ($a_{CDOM}300$) decreased for all sites during the combined photobleaching and microbial degradation treatment, but to a much greater extent (by 56.0% over 7 days on average, SD = 4.3%), ranging from a loss of 48.4% at the SERC Dock in July 2018 to 63.1% at Sweet Hall in January 2017 (Figures 6b and 7b). There was little variation in the change in $a_{CDOM}300$ across the estuarine gradient or between marshes ($P > 0.05$). There was, however, a seasonal dependence, with a significantly higher relative loss in $a_{CDOM}300$ in January (59.5% over 7 days, on average, SD = 3.1%) compared to July (52.5% over 7 days, on average, SD = 3.1%) ($P < 0.01$). S_R showed a consistent and significant increase (by 94.8% over 7 days for all sites on average, SD = 27.9%, $P < 0.01$), as a result of an increase in $S_{275–295}$ and a

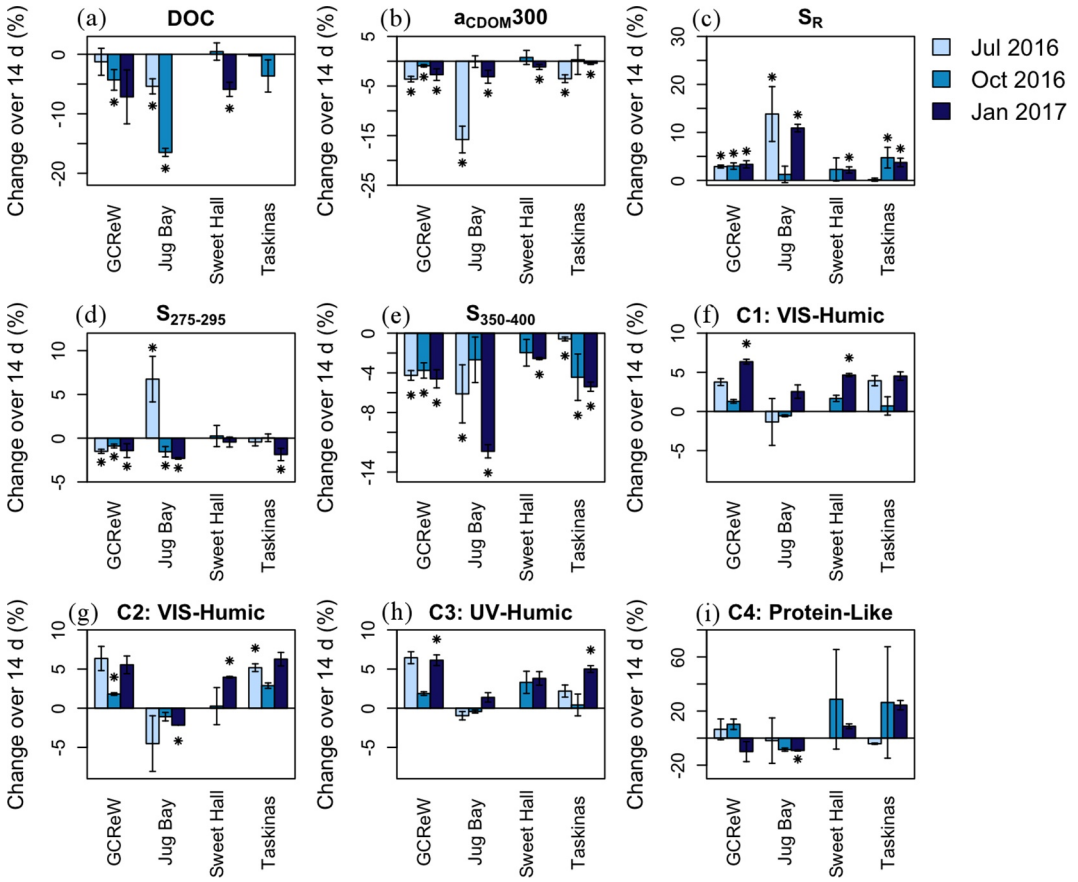

Figure 5. Change in DOC concentration (a) and CDOM optical properties (b-i) over 14 days of dark incubations performed on GF/F filtrate during July 2016, October 2016, and January 2017. Error bars represent the standard deviation between replicate bottles. Asterisks represent a significant difference between the percent change and zero (*t*.test, $P < 0.05$).

decrease, or no change, in $S_{350–400}$ (Figures 6b and 7e). Across the Rhode River estuarine gradient, the greatest percent increase in S_R occurred at Upper Muddy Creek (83.7% over 7 days), with a monotonic decrease in S_R change downstream toward the mouth (Figure 6b). The percent increase in S_R was also significantly higher in the winter compared to the fall and summer and in the fall compared to the summer ($P < 0.01$) (Figure 7c). Jug Bay had a greater increase in S_R (129.8% over 7 days, on average, SD = 16.3%, $P < 0.01$) and GCReW an overall smaller increase in S_R (88.2% over 7 days, on average, SD = 15.7% $P < 0.01$). The increase in $S_{275–295}$ was significantly greater at Taskinas than both Jug Bay and Sweet Hall ($P < 0.01$). Furthermore, there was a significantly lower percent increase in $S_{275–295}$ in the summer compared to the fall and winter ($P < 0.01$) (Figure 7d). Jug Bay and GCReW also had a significantly greater (29.6% over 7 days, on average, SD = 4.1%) and lower (13.1% over 7 days, on average, SD = 3.0%) percent loss in $S_{350–400}$, respectively, than the other sites ($P < 0.01$), except for Taskinas which showed no significant difference compared to GCReW ($P > 0.05$).

Combined photobleaching and microbial degradation resulted in a significant decrease in all the humic-like fluorescence components ($P < 0.01$), with the greatest losses occurring in the shorter-wavelength VIS-humic-like component (C1) and the marine-humic-like component (C3) (Figures 6e, 7f and 7h). For the Rhode River sites, the percent loss of C1 was greatest in terrestrially sourced sites such as Upper Muddy Creek (loss of 79.5% over 7 days). This loss decreased down-estuary, with the lowest percent loss occurring at the Rhode River Mouth (loss of 63.2% over 7 days). The decrease in C1 and C3 was significantly lower at the GCReW marsh compared to Upper Muddy Creek, the "non-marsh terrestrial" site ($P < 0.01$). Furthermore, Upper Muddy Creek had a significantly greater percent loss in all humic-like components (C1, C2, and C3) compared to the other sites ($P < 0.01$). GCReW also had a significantly lower percent loss of the three

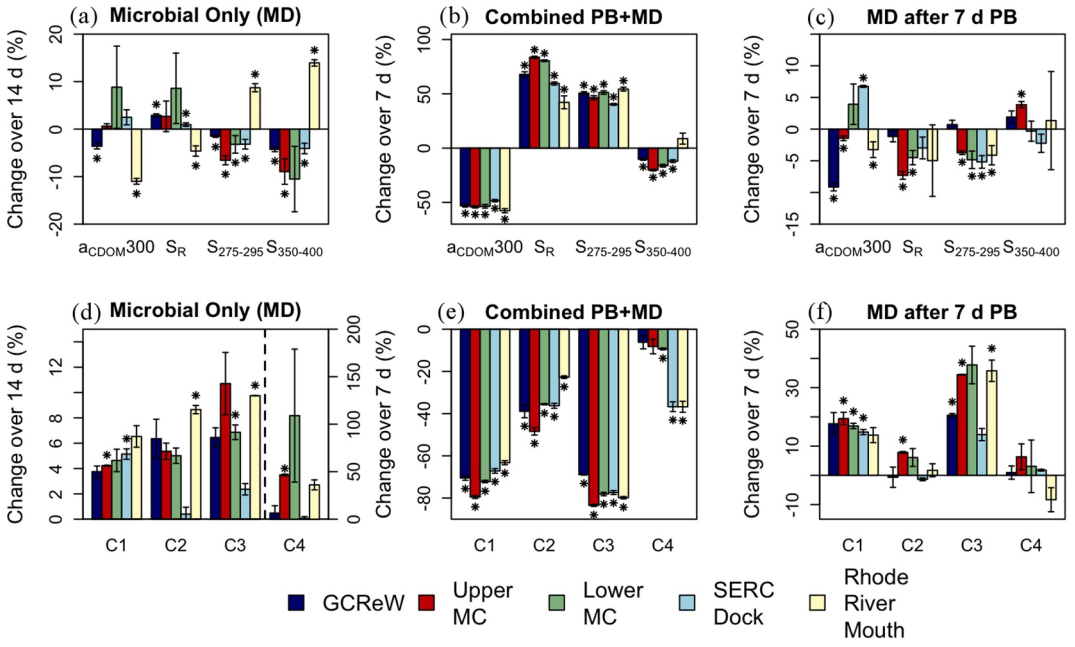

Figure 6. Changes to CDOM absorption properties (a, b, and c) and CDOM fluorescence properties (d, e, and f) for the microbial-only treatment (a and d), the combined photobleaching and microbial treatment (b and e), and the microbial treatment after 7 days of photobleaching (c and f) for the Rhode River sub-estuary sites. Sites are ordered along the salinity gradient, starting with the marsh end-member (GCReW) and ending with the estuarine end-member (Rhode River Mouth). The C4 component in the microbial-only treatment (d) is plotted on a different scale than the other three components. Error bars represent the standard deviation between replicate bottles. Asterisks represent a significant difference between the percent change and zero (*t*.test, $P < 0.05$).

Table 4
Average Percent Change for All Incubations and Sites (Marsh and Rhode River), for Each Measured Parameter

Treatment	Site n[a]	$a_{CDOM}300$	S_R	$S_{275–295}$	$S_{350–400}$	C1	C2	C3	C4
MD (14 days)	Marsh	−2.8%	4.4%	−0.3%	−4.4%	2.5%	2.2%	2.7%	6.5%
	43, 22	(4.6%)	(4.5%)	(2.6%)	(3.1%)	(2.4%)	(3.8%)	(2.5%)	(19.2%)
	RR	−0.5%	2.1%	−1.1%	−2.8%	4.9%	5.2%	7.2%	39.8%
	20, 10	(7.7%)	(5.4%)	(5.4%)	(9.4%)	(1.1%)	(2.9%)	(3.2%)	(47.1%)
PB + MD (7 days)	Marsh	−57.0%	105.1%	63.3%	−19.6%	−79.1%	−51.2%	−78.6%	−8.3%
	33, 22	(4.1%)	(23.4%)	(8.7%)	(7.6%)	(4.3%)	(6.0%)	(5.4%)	(23.0%)
	RR	−53.4%	66.7%	48.6%	−10.0%	−70.5%	−36.4%	−77.5%	−19.4%
	15, 10	(3.3%)	(15.8%)	(5.2%)	(10.5%)	(5.8%)	(8.8%)	(5.1%)	(15.0%)
MD after PB (7 days)	Marsh	−6.0%	−3.7%	−0.4%	3.7%	17.9%	−1.8%	18.8%	3.6%
	33, 21	(6.3%)	(5.0%)	(4.0%)	(5.0%)	(8.5%)	(6.6%)	(11.8%)	(12.6%)
	RR	−0.6%	−4.2%	−3.4%	0.9%	16.5%	2.7%	28.5%	0.8%
	15, 10	(5.9%)	(3.1%)	(2.4%)	(3.7%)	(2.7%)	(4.2%)	(10.3%)	(6.4%)

Note. The four marsh sites in Figure 2a averaged across all three seasons for "Marsh," with the exception of Sweet Hall in the summer of 2016, which was not sampled. The five Rhode River sites in Figure 2b, including GCReW, averaged during the summer of 2016 for "RR." Negative values indicate a net loss and positive values a net gain. Standard deviations are listed in parentheses.

GCReW, Global Change Research Wetland.

[a]The total number of samples, including incubation replicates, averaged for the absorption indices and fluorescence indices, respectively.

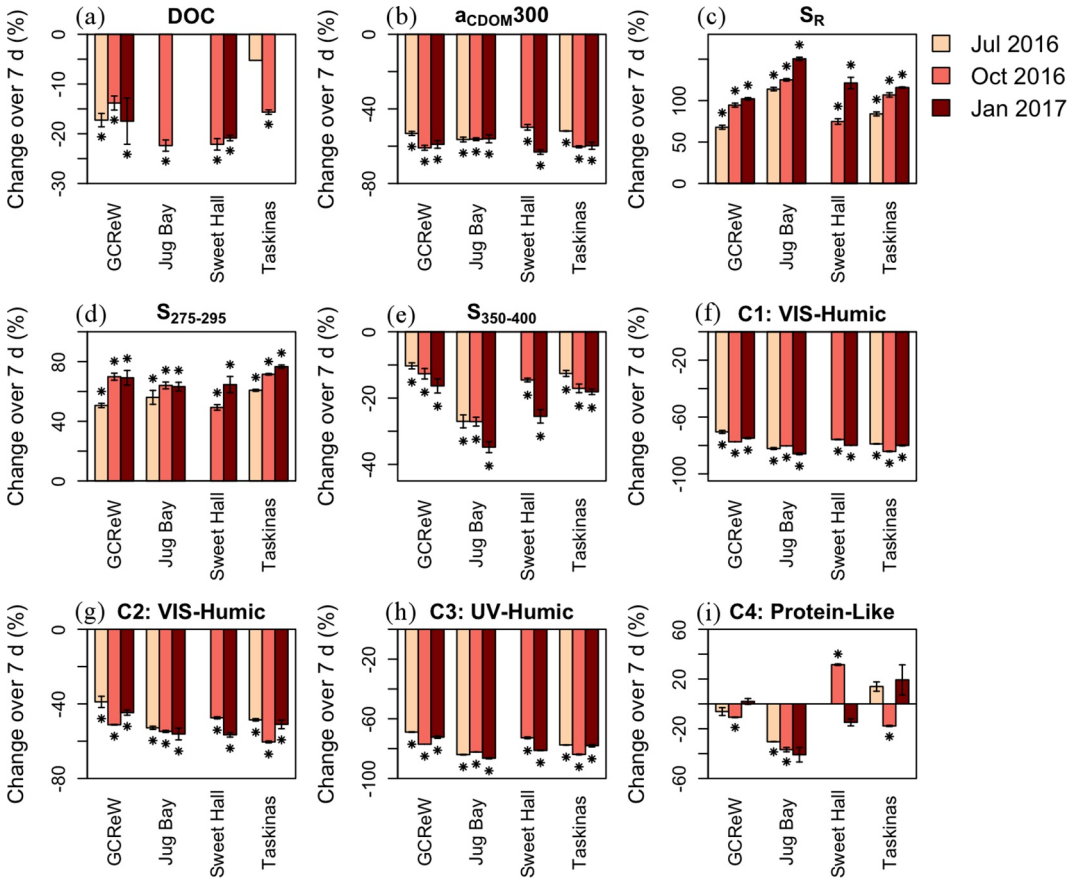

Figure 7. Change in DOC concentration (a) and CDOM optical properties (b-i) over 7 days of light incubations performed on GF/F filtrate (combined photobleaching and microbial, "PB + MD") during July 2016, October 2016, and January 2017. Error bars represent the standard deviation between replicate bottles. Asterisks represent a significant difference between the percent change and zero (*t*.test, $P < 0.05$).

humic-like components compared to Jug Bay and Taskinas ($P < 0.05$). In general, the protein-like component (C4) varied more than the humic-like components. There was a consistent decrease in C4 with combined photobleaching and microbial degradation at Jug Bay, in all seasons (Figure 7i) ($P < 0.1$).

3.5. Effects of Photobleaching on Microbial Degradation

DOC decreased for all marsh sites by, on average, 5.9% (SD = 5.6%) over the 7-day dark incubation after light exposure (Table 4 and Figure 8a); this was greater than the loss of DOC from microbial degradation alone, which was 5.5% (SD = 5.4%) over the twice as long period of 14 days. There were no significant differences in DOC loss between sites or seasons ($P > 0.05$).

The average decrease in $a_{CDOM}300$ for the marsh sites was 6.0% (SD = 6.3%) over the 7-day dark incubation after photobleaching, which is considerably larger than the average decrease of 2.8% (SD = 4.6%) over the longer 14-day microbial-only incubations (Table 4). Jug Bay had a significantly greater loss in $a_{CDOM}300$ compared to the other marsh sites (marginal means 13.7% vs. 0.5%–6.0% over 7 days, RSE = 3.5%, $P < 0.01$) (Figure 8b). Contrary to the microbial-only and combined photochemical and microbial incubations where S_R increased, in the microbial degradation incubations after photobleaching S_R consistently decreased by, on average, 4.2% (SD = 3.1%) for the Rhode River sites and 5.8% (SD = 2.9%) for the marsh sites (Table 4). This decrease in S_R was mostly the result of a decrease in $S_{275–295}$ and an increase in $S_{350–400}$. CDOM from the Jug Bay marsh, however, showed different results, with both $S_{275–295}$ and $S_{350–400}$ increasing during the microbial incubation after photobleaching, except in July 2016 when $S_{350–400}$ decreased, resulting in an increase in S_R (Figures 8c and 8e).

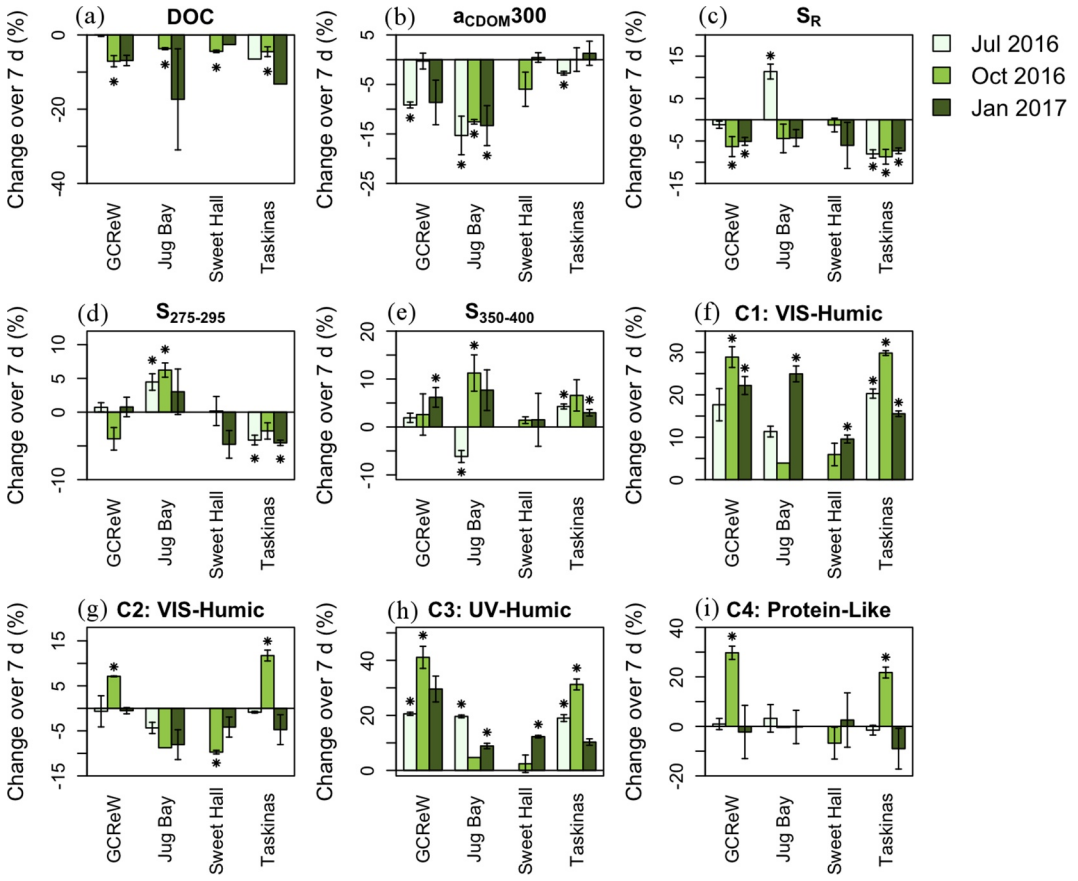

Figure 8. Change in DOC concentration (a) and CDOM optical properties (b-i) over 7 days of dark incubations after 7 days of light incubations performed on GF/F filtrate during July 2016, October 2016, and January 2017. Error bars represent the standard deviation between replicate bottles. Asterisks represent a significant difference between the percent change and zero (*t*.test, $P < 0.05$).

Overall, exposure to light increased the subsequent microbial production of CDOM fluorescence (Figures 8f–8i), especially for the humic-like peaks C1 and C3 that both consistently increased with microbial degradation after photobleaching to a greater extent than by microbial degradation alone. Specifically, 7 days of microbial degradation following 7 days of photobleaching resulted in an increase in C1 by 16.5% (SD = 2.7%), on average, in the Rhode River sites and by 17.9% (SD = 8.5%) in the marsh sites (Table 4). This is considerably higher than the 4.9% (SD = 1.1%) and 2.5% (SD = 2.4%) increase for estuarine and marsh sites, respectively, in the 14-day microbial-only incubations. Similarly, component C3 increased by 28.5% (SD = 10.3%) for the Rhode River sites and by 18.8% (SD = 11.8%) for the marsh sites, compared to just 7.2% (SD = 3.2%) and 2.7% (SD = 2.5%) increase, respectively, in the 14-day microbial-only incubations. C4 was much more variable, with most incubations showing no significant changes ($P > 0.1$).

Along the estuarine gradient, the UV-humic-like peak C3 showed overall the largest increase with microbial degradation after photobleaching, both for the terrestrial (Upper and Lower Muddy Creek) and the estuarine (Rhode River Mouth) end-members (Figure 6f). The VIS-humic-like peak, C1, also showed a consistent increase with microbial degradation after photobleaching that monotonically decreased, however, with increasing salinity along the estuary.

4. Discussion

4.1. CDOM Properties at the Wetland-Estuary Interface

Our measurements in the Rhode River system showed a decreasing gradient in highly absorbing CDOM and humic-like fluorescence with increasing distance from the marsh and watershed. These gradients are driven by dilution of terrestrial (including marsh) CDOM sources, as well as removal, production and transformation of CDOM within the estuary. The steeper gradient of the two visible humic-like fluorescence components (C1 and C2) compared to the UV-humic-like (C3) and protein-like (C4) components from the GCReW marsh to the Rhode River mouth initially (Table 3) indicate either preferential loss of the longer wavelength, higher molecular weight humic-like components relative to C3 and C4 or additional sources of C3 and C4 down-estuary. Since C3 and C4 are both associated mostly with microbially processed material (Coble, 1996; Fellman et al., 2010) and C1 and C2 are associated mostly with terrestrial sources (Coble, 1996; Fellman et al., 2010; Wagner et al., 2015; Yamashita et al., 2010), it is likely that C3 and C4 fluorescence down-estuary is supplemented by relatively stronger autochthonous production. This is consistent with the results from our microbial incubation experiments showing a larger increase in C3 and C4 fluorescence relative to C1 and C2 for both estuarine and marsh-exported CDOM (MD treatment, Table 4). Moreover, C3 fluorescence showed the largest increase in our microbial incubations after photobleaching (MD after PB treatment, Table 4).

The decrease in $a_{CDOM}300$ (by more than a factor of 3) and increase in S_R (from 1.03 to 1.49) with distance from the marsh endmember suggests a decrease in the molecular weight and aromaticity of CDOM across this marsh-estuarine gradient (Table 3), in agreement with other studies (Dalzell et al., 2009; Fellman et al., 2011; Helms et al., 2008; Hernes, 2003; Tzortziou et al., 2011, 2008; Yamashita et al., 2008). For samples collected along a transect in the Delaware Estuary, Helms et al. (2008) proposed that the optics down-estuary were the result of: the mixing of low S_R (terrestrial) CDOM with high S_R (autochthonous or photobleached terrestrial) CDOM, increasing $S_{275–295}$ down-estuary (photobleaching impacts), and decreasing $S_{350–400}$ down-estuary (microbial impacts). While the salinity gradient in Helms et al. (2008) had a much larger range than the Rhode River (i.e., 0–40 vs. 6–9 salinity), nonconservative mixing in CDOM optical properties such as $a_{CDOM}440$ and $S_{290–750}$ was previously reported for the Rhode River along transects from the marsh endmember to the mouth of the estuary (Tzortziou et al., 2011), suggesting a sink for highly absorbing CDOM. J. B. Clark et al. (2020) showed this sink to be phototransformation; they estimated that about half of the total DOC input from the marsh and watershed to the Rhode River is photochemically transformed to a more biologically labile (and less absorbing) DOC pool. Therefore, in the summer, the GCReW marsh exports high molecular weight (low S_R) and strongly absorbing (high $a_{CDOM}300$) CDOM to the surrounding estuary (Tzortziou et al., 2008, 2011). The marsh-exported CDOM is then photobleached and microbially degraded (J. B. Clark et al., 2020), mixed with terrigenous CDOM from Muddy Creek, and diluted with down-estuary water characterized by lower $a_{CDOM}300$ and higher S_R (Tzortziou et al., 2011).

Consistent CDOM quality in the Rhode River estuary inter-annually suggests consistent CDOM sources and transformation pathways. Our measured S_R of 0.92 at GCReW and 1.27 at the SERC Dock in July 2016 were remarkably consistent with the S_R values of 0.9 at GCReW and 1.29 at the SERC Dock reported for July 2008 measurements in Tzortziou et al. (2011). These observations, conducted in same season and tidal stage but different years, suggest consistency in the relative contribution of different CDOM sources and transformation pathways across this marsh-estuarine gradient. Tzortziou et al. (2008), measured $a_{CDOM}300$ of 35.7 m^{-1} and 54.2 m^{-1} (both having absorption spectral slopes $S_{290–750}$ of 0.0143 nm^{-1}) for two asymmetrical low-tides (i.e., GCReW-exported CDOM) on July 2004. While one of these values is similar to our measurement of 36.7 m^{-1} for $a_{CDOM}300$ at GCReW in July 2016, the other is not. Ultimately, this demonstrates that while down-estuary gradients of optical parameters that are proxies for CDOM composition (i.e., S_R, $S_{290–750}$) remain overall consistent, the magnitude of proxies that are driven by both CDOM amount and composition (i.e., $a_{CDOM}300$) vary on interannual, seasonal, and even daily timescales, especially during asymmetrical tidal cycles (Tzortziou et al., 2008).

4.2. CDOM as a Function of Source and Season

Across the marsh sites, DOC concentrations, $a_{CDOM}300$, and contributions of the four PARAFAC fluorescence components decreased from July to January, in some cases by a factor of two or more, thus indicating greater marsh export of carbon-rich, more absorbing and strongly fluorescent CDOM in the summer compared to the winter (Table 3). Similar seasonal changes have been reported in previous studies (Fellman et al., 2008; Osburn et al., 2015; Shultz et al., 2018; Stedmon & Markager, 2005; Tzortziou et al., 2008). Seasonally, the contributions of various CDOM sources at the marsh-estuary interface may vary; for example, in the winter compared to the summer, there is likely a lesser contribution of CDOM from marsh plant leachates; however, DOM contributions of from fresh plant materials in other marsh systems have been shown to be minor relative to soil (C. D. Clark et al., 2008). Moreover, due to the temperature-dependence of soil CDOM export in similar systems such as rivers (Shultz et al., 2018), the contribution of wetland-soil CDOM is also likely lower in the winter. Since CDOM absorption and fluorescence quality indices (ratios of fluorescence components, $S_{R,}$ and $S_{275-295}$), showed considerably smaller changes seasonally and inter-annually relative to the quantity of marsh DOM export, it is likely that marsh-exported CDOM mostly originates from marsh soil porewater rather than plant leachates, as suggested in C. D. Clark et al. (2008). The gradual release of DOM stored in tidal marsh soils reduces much of the seasonal and inter-annual variability in the quality of DOM exported from temperate marshes relative to the strong seasonal and inter-annual variability in the ultimate source of these compounds (i.e., plant biomass), thus buffering marsh DOM export.

Dominated primarily by non-persistent emergent vegetation and downstream of a major WWTP, Jug Bay differed from the other marsh systems in both CDOM quantity and composition. In the winter, Jug Bay had much lower CDOM absorption and fluorescence (expressed by $a_{CDOM}300$ and C1) compared to the other marshes. This is likely the result of the lack of emergent vegetation at Jug Bay during the winter and a smaller peat reserve and greater mineral content compared to the other marshes (Pinsonneault et al., 2020; Swarth et al., 2013). In addition, the observed high contributions of marine-humic-like and protein-like CDOM fluorescence components at Jug Bay compared to the other marshes indicates a greater contribution of microbial CDOM and could be representative of the influence of wastewater treatment effluent at this site, given that the marine humic-like component has been shown to be higher in sewage and wastewater (Guo et al., 2010). Thus, Jug Bay exemplifies the role of both source material (e.g., vegetation type and soil characteristics) as well as environmental characteristics, such as water quality, on CDOM quantity and composition.

4.3. Microbial Impacts in the 0.2 μm Fraction

Many incubation studies assume little to no microbial activity in 0.2 μm filtrate, despite studies demonstrating the 0.2 μm filterability and growth of certain microbial communities in experiments even though sterilization of equipment was performed (Liu et al., 2019; Wang et al., 2008). In fact, significant microbial presence in 0.2 μm filtrate has been observed in inland surface waters (Brailsford et al., 2017; Elhadidy et al., 2016; Wang et al., 2007), coastal water (MacDonell & Hood, 1982; Obayashi & Suzuki, 2019), and groundwater (Luef et al., 2015). Our results showed that while microbial counts in the 0.2 μm filtrate were about an order of magnitude lower than the GF/F filtrate before the incubation, they approached those in the GF/F filtrate after only 2 days (Figure 3), suggesting the potential for microbial interference in a filtrate that is often assumed to be "sterile." Microbial counts reported here for 0.2 μm filtrate are similar to those reported for other aquatic systems such as freshwater lakes and rivers (Liu et al., 2019; Wang et al., 2007). The interference of microbes was further supported by the observed similar trends between the "control" 0.2 μm 14-day dark incubation and the MD-only 14-day incubation.

While UV exposure has also been assumed to inhibit microbial growth, in our incubations low-level UV light exposure that was mainly composed of long-wavelength UV-A did not inhibit microbial growth as evidenced by the small difference between the dark and light microbial counts at the end of the 7-day incubation ($P > 0.1$) (Figure 4). Therefore, the potential for microbial interference in treatments that are assumed to isolate the impacts of other degradation processes, such as photobleaching, must be acknowledged. Work addressing potential solutions to bacterial contributions in commonly used "sterile" fraction sizes (i.e., 0.2 μm) should be conducted, and microbial counts should be measured for incubations when possible. Common treatment methods to inhibit microbial growth, for example sodium azide, can interfere

with CDOM optical measurements (Retelletti Brogi et al., 2019) and thus can't be used for photobleaching-only experiments that are assessing changes to CDOM optics. Incubations that assume 0.2 μm fractions as "sterile" without the presentation of microbial cell counts or similar evidence of sterility should be interpreted with caution, as there exists the potential for under- or over-estimation of degradation processes such as photobleaching, due to the coupled effects of microbial activity. Photodegradation experiments conducted on very short-time scales may reduce the confounding effects of microbial growth, and thus should be considered, when possible.

4.4. Photobleaching Increases CDOM Bioavailability

Microbial degradation of DOM is affected by numerous factors, such as nutrient availability, microbial community composition, source material, previous light exposure, and temperature (which was constant in our experiments); thus, the effects of microbial degradation on marsh-exported CDOM were highly variable. This variability is particularly apparent when comparing across marshes and seasons. In general, microbial degradation resulted in increases to CDOM humic-like and protein-like (C4) fluorescence (Figures 5f–5i, 6d, 6f, and 8f–8i), but decreases to CDOM absorption (Figures 5b, 6a, 6c, and 8b). Similar to other studies, we observed a small (within 10%, Table 4, Figures 5f, 5h, and 6d) increase in the shorter-wavelength VIS- and marine-humic-like fluorescence components (C1 and C3) of marsh and estuarine CDOM with microbial degradation alone (Cory et al., 2015; Lu et al., 2013; Moran et al., 2000; Rochelle-Newall & Fisher, 2002), particularly for C3, which is associated with biological processing. This increase could be the biological transformation of non-colored DOM to colored DOM, as hypothesized by Rochelle-Newall and Fisher (2002). The observed down-estuary increase in C1 microbial production could be due to the increasing presence of algal-derived DOM down-estuary, which has been proposed as the non-colored DOM substrate converted into the colored, humic-like CDOM fluorescence fraction (Rochelle-Newall & Fisher, 2002). The greater increase in C1 microbial production down-estuary could also be due to greater prior light exposure during transport down-estuary, and therefore, a greater CDOM bioavailability.

Previous exposure to light increased the bioavailability of CDOM at all sites, resulting in a greater loss of both DOC and $a_{\mathrm{CDOM}}300$ and a greater production of humic-like CDOM over a shorter incubation time (7 vs. 14 days for the microbial-only incubation). Similar results have been reported for the Ria de Aveiro estuary (Santos et al., 2014), the Satilla estuary dominated by vascular plant CDOM inputs (Moran et al., 2000), and an arctic headwater stream (Cory et al., 2015). The bioavailability increase was particularly prominent in sites where the contributions of terrestrial, humic-like, and aromatic CDOM were higher, and with less previous exposure to UV-radiation; for example, the bioavailability increase in C1 was greater in the marsh and watershed sites (GCReW and the Upper Muddy Creek) compared to the down-estuary sites, since estuarine CDOM has likely undergone substantially more photobleaching (Tzortziou et al., 2007). Microbial production of C3 increased the most after photobleaching, particularly in the Rhode River sites. Without previous exposure, microbial production of C3 was only slightly higher than that of C1 (7.2% compared to 4.9% over 14 days for the Rhode River sites); after photobleaching, however, the increase in C3 during microbial degradation was, on average, almost double that of C1 (28.5% compared to 16.5% over 7 days for the Rhode River sites). Therefore, while photobleaching stimulates the microbial production of both C1 and C3, the relative increase in C3 is greater. For the marsh sites, the loss of C2 during microbial degradation after photobleaching was significant, even in sites that showed no loss with microbial degradation alone; this indicates that photobleaching is allowing for the microbially mediated decrease of C2 fluorescence. While fluorescence components C1, C2, and C3 (humic-like) are often described as terrestrially sourced and associated with wetlands (which they often are, including in the marshes studied here), our results, consistent with other studies (Medeiros et al., 2017; Tanaka et al., 2014), demonstrate another source in estuarine systems: microbial production within the estuary.

In general, CDOM absorption ($a_{\mathrm{CDOM}}300$) decreased with microbial degradation. This is consistent with other incubations of terrestrial CDOM (Cory et al., 2015; Moran et al., 2000; Santos et al., 2014), though increases in CDOM absorption for estuarine and marine CDOM have also been reported (Miller & Moran, 1997; Nelson et al., 2004; Rochelle-Newall & Fisher, 2002; Santos et al., 2014). The observed loss in $a_{\mathrm{CDOM}}300$ during microbial processing was enhanced by previous exposure to light, with a loss of 2.8% over 14 days in the microbial-only treatment, and 6.0% over half the time (7 days) during the microbial incubation with

prior photobleaching. This is consistent with Miller and Moran (1997), where CDOM from a coastal salt marsh dominated by *Sporobolus alterniflora* showed no change in $a_{CDOM}350$ by microbial degradation alone but a 4% decrease by microbial degradation after photobleaching. On the other hand, in an arctic headwater stream dominated by terrestrial soil CDOM sources, CDOM absorption and fluorescence increased during microbial incubations after photobleaching (Cory et al., 2015). These differences indicate the importance of CDOM source when evaluating the impacts of photobleaching on microbial degradation.

4.5. Factors Influencing CDOM Photoreactivity

Our combined photobleaching and microbial incubations highlighted the dominant role of photobleaching, but also the importance of simultaneous microbial processing, in shaping certain CDOM optical properties in estuarine waters. The substantial loss of all three humic-like fluorescence components and $a_{CDOM}300$ (by > 50%, Table 4) in the PB + MD treatment is consistent with previous studies on the impacts of photobleaching alone (Aulló-Maestro et al., 2016; Cory et al., 2015; Helms et al., 2008; Tzortziou et al., 2007), indicating the dominant role of photobleaching as the main CDOM quality transformation mechanism for the specific samples. This is further supported by the much larger change in all CDOM optical properties over the 7-day combined incubation compared to the microbial treatments with and without previous light exposure. Yet, the influence of microbial degradation in the combined treatments may still be important, especially for some parameters. Although both microbial and photochemical degradation decreased marsh and estuarine CDOM absorption, photobleaching resulted in opposite shifts in CDOM fluorescence, with humic-like components decreasing during photochemical degradation and increasing during microbial processing. The increase in humic-like CDOM fluorescence (i.e., C1 and C3) during microbial degradation after prior photobleaching was substantial compared to the fluorescence loss during the combined photobleaching and microbial treatment (Table 4), especially compared to the differences between sites and seasons (Figure 6e compared to Figures 6f and 7f–7h compared to Figures 8f–8h). Therefore, the loss of the humic-like fluorescence in the combined photobleaching and microbial treatment is likely much lower than it would be for photobleaching alone, given the offset in loss due to the simultaneous microbial production; furthermore, trends in the humic-like fluorescence components during the combined photochemical and microbial treatment cannot be confidently attributed to photobleaching alone, and thus the change in humic-like fluorescence in this study may not be a good proxy for the amount of photobleaching. S_R, on the other hand, was both the parameter that changed the most during photobleaching and was also not as highly impacted by microbial degradation (Table 4). In fact, the amount of change in S_R during microbial degradation after previous light exposure was in many cases less than the difference between sites or seasons in the combined photochemical and microbial treatment (Figure 6b compared to Figures 6c and 7c compared to Figure 8c). Thus, the change in S_R may be a good proxy to gauge the amount of photobleaching, despite the simultaneous influence of microbial processing.

CDOM photoreactivity is driven by both CDOM source and prior light exposure. For the Rhode River, the greatest increase in S_R occurred in the terrestrial sites, where the contributions of CDOM with presumed higher aromaticity (GCReW, Upper and Lower Muddy Creek) were greatest; the lowest increase occurred in the estuarine end-member (Rhode River Mouth) (Figures 6b and 6e), which had the lowest contribution of terrestrial CDOM due to dilution, transformation, and removal. Previous exposure of CDOM to solar radiation during transport from the head to the mouth of the Rhode River also plays a role in the decrease in CDOM photoreactivity along the estuarine gradient (Tzortziou et al., 2007). In addition to longer exposure time with transit along the salinity gradient, the water clarity at down-estuary sites is greater (Rose et al., 2018), allowing for greater exposure to sunlight (and thus lower photoreactivity) compared to more turbid waters closer to terrestrial margins. The greater photoreactivity of the Upper Muddy Creek ("non-marsh terrestrial") compared to GCReW ("marsh") is also likely impacted both by differences in CDOM source, as well as differences in previous UV-exposure. Canopy cover along the Upper Muddy Creek creates a more shaded environment compared to GCReW; this has been observed in other systems, such as streams, where an increase in canopy cover was associated with an increase in CDOM photoreactivity (Lu et al., 2013). In addition, water clarity in Muddy Creek is very low due to a high suspended matter concentration, which results in less CDOM exposure to sunlight (Rose et al., 2018). On the other hand, differences in turbidity between marsh tidal creeks did not explain the differences in photoreactivity that we observed

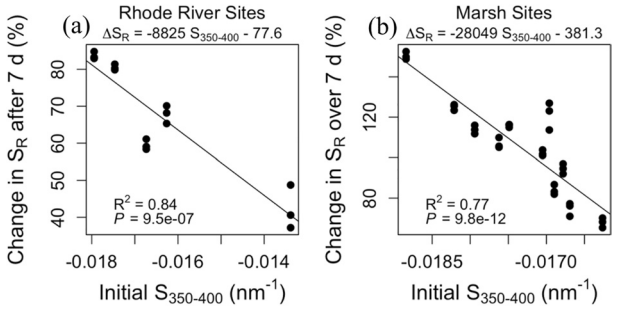

Figure 9. Initial $S_{350–400}$ as a predictor of combined photobleaching and microbial degradation, defined as the change in S_R over the 7-day light incubation, for (a) the Rhode River sites and (b) the marsh sites.

across marsh sites (data not shown). Thus, any differences in photoreactivity between the marsh sites studied here was mostly driven by differences in DOM source.

The photoreactivity of marsh-exported CDOM showed small but statistically significant seasonal trends. There was an overall smaller relative change in $a_{CDOM}300$, $S_{275–295}$, and S_R during the summer compared to the winter (Figures 7b–7d). The observed seasonality in the change in $a_{CDOM}300$, $S_{275–295}$, and S_R, and therefore, photobleaching, is likely driven both by the small differences in the relative contributions of various marsh-CDOM sources seasonally as well differences in UV-exposure prior to collection. Greater relative contributions of fresh marsh plant leachate in the summer, which has previously been shown to have a lower photoreactivity relative to soils (Chen & Jaffé, 2014), could partially explain why photoreactivity was lower in the summer relative to the winter, even if the contributions are small (C.D. Clark et al., 2008). Less prior exposure to UV-radiation in January, due to a lower sun angle, greater cloudiness, and shorter days, could also contribute to the greater CDOM photoreactivity in the winter compared to the summer. Previous studies in temperate streams and lakes showed that UV-radiation history was the main factor dictating photoreactivity for CDOM of similar source material (Cory et al., 2015; Lu et al., 2013; Osburn et al., 2001).

None of the initial optical properties predicted the observed spatiotemporal variability in CDOM photoreactivity, estimated as the change in S_R, except $S_{350–400}$ (Figure 9). The initial $S_{350–400}$ was the best predictor of photoreactivity for both the various sites within the Rhode River ($R^2 = 0.84$, $P < 0.01$) (Figure 9a), across different marsh systems ($R^2 = 0.77$, $P < 0.01$) (Figure 9b), and both datasets combined ($R^2 = 0.73$, $P < 0.01$, data not shown). Other studies, based on water samples collected across a wide range of water types, have suggested that $S_{350–400}$ is a good proxy of CDOM molecular weight (Helms et al., 2008). Given that the change in $S_{350–400}$ by photobleaching is lower than the change in other absorption parameters such as $S_{275–295}$ (5%–25% vs. 60%–80%), $S_{350–400}$ could act as a proxy for the combined effects of both the original molecular weight of the source as well as previous UV exposure. While the history of photobleaching will impact the photoreactivity of CDOM, and these impacts are most easily observed in changes to $S_{275–295}$, we observed little variation in the change in $S_{275–295}$ across sites, even across sites with very different CDOM characteristics initially (Table 3, Figures 6b, and 7d); however, the change in $S_{350–400}$ by photobleaching is directly related to differences in initial CDOM quality between sites (Table 3, Figures 6b, and 7e). As such, it could be argued that $S_{350–400}$ is better at predicting photoreactivity in both photobleached systems (Rhode River sites) as well as at sites with relatively un-altered CDOM (marsh and watershed sites), compared to other parameters that are more highly influenced by photobleaching. Interestingly, for predicting DOC loss for combined photobleaching and microbial degradation, $S_{350–400}$ was not a good predictor; instead, $a_{CDOM}300$ showed the best correlation out of all the measured optical parameters ($R^2 = 0.45$, $P < 0.01$, data not shown). While the combined photoreactivity and bioavailability of the winter CDOM was greater than the summer CDOM, both photobleaching and microbial degradation are likely more important CDOM removal processes in the summer due to higher levels of UV-radiation and higher summer water temperatures. UV-radiation exposure and temperature in our study were kept constant across samples despite these seasonal differences.

4.6. Jug Bay Exports Extremely Bioavailable and Photoreactive CDOM

Compared to other systems, the loss of both $a_{CDOM}300$ and DOC at Jug Bay over the 14-day microbial-only incubation was high, indicating particularly high bioavailability. Lu et al. (2013) reported DOC losses of 1%–9% for 35–36 day incubations of stream DOM, under similar experimental conditions; Moran et al., (2000) showed a DOC loss of 2.9% over their 51-day dark incubation. In our study, DOC from the Jug Bay system decreased on average by 11.7% over 14 days in the MD treatment, which is less than half the incubation time in Lu et al. (2013) and 3 times less than Moran et al., (2000). Moreover, for our microbial-only treatment, CDOM collected from Jug Bay showed only a small change in two of the humic-like components, C1 and C3, and a decrease in the longer-wavelength VIS- humic-like component, C2 (Figures 5f–5h), compared to the increases in C1, C2, and C3 observed in all other marsh sites. This could indicate either the lack of

production of the humic-like components as seen in the other sites, or, the simultaneous microbial utilization and degradation of humic-like fluorescence, thus offsetting its production. Given that Jug Bay also had a much higher loss in $a_{CDOM}300$ and DOC, a greater increase in S_R, and a greater decrease in $S_{350–400}$ during the microbial-only incubations compared to the other sites, it is likely that the microbially produced, humic-like CDOM at Jug Bay is particularly bioavailable, and thus is being utilized and degraded quickly.

The Jug Bay marsh system also exports highly photoreactive CDOM. The consistent loss of protein-like CDOM fluorescence across all seasons at Jug Bay in the combined photobleaching and microbial degradation treatment indicates that the protein-like CDOM at Jug Bay is more photoreactive than at the other sites that showed a general increase in C4 (Figure 7i). In addition, Jug Bay had a significantly greater increase in S_R and a greater loss in $S_{350–400}$ with light exposure than the other sites, further supporting higher rates of photobleaching.

5. Conclusions

Through a complex interplay of physical and biological processes, marsh-estuary ecosystems are important sources, reactors, and transformers of dissolved organic carbon and nutrients, regulating biogeochemical exchanges along terrestrial-aquatic interfaces. Using a combination of field measurements and laboratory incubations, our study captured the impact of photochemical and microbial processes on marsh-exported CDOM across different seasons and systems characterized by different vegetation properties, water quality, and salinity regimes. Photobleaching is mostly determined by the absorptivity, molecular weight, and aromaticity of the CDOM, as well as previous exposure to UV-radiation; for our samples, the potential for photobleaching was best estimated using $S_{350–400}$. In the summer, when concentrated, high-molecular-weight, and aromatic marsh-exported CDOM received maximum exposure to UV-radiation, photobleaching was an important process for CDOM transformation and, subsequently, microbial degradation (J. B. Clark et al., 2019). CDOM photoreactivity decreased down-estuary away from the marsh endmember, with increasing prior exposure and with a greater contribution of marine-derived CDOM relative to terrestrially derived CDOM. While marsh-export of CDOM and DOC showed a strong seasonal cycle, with greater export in the summer, optical proxies for CDOM quality (e.g., S_R and fluorescence PARAFAC ratios C2/C1, C3/C1, and C4/C1) showed considerably less seasonal and interannual variability, suggesting the soil-buffering of marsh-DOM export. Marsh-exported CDOM photoreactivity showed small but statistically significant seasonal dependence, with greater photoreactivity measured on CDOM collected in the winter compared to the summer. Under natural conditions, lower UV radiation in winter is expected to result in considerably less photochemical (and, thus, also microbial) degradation of marsh-exported CDOM down-estuary. This suggests a greater relative contribution of photoreactive, allochthonous CDOM down-estuary in the winter compared to the summer.

Because microbial degradation has been shown to both degrade absorbing and fluorescing CDOM and produce fluorescing CDOM, the net effect of microbial processing on CDOM optical properties can vary depending on the available substrate (Tranvik, 1988, 1993; Volk et al., 1997), nutrients, temperature (Lønborg et al., 2009), bacterial communities (Kirchman et al., 2004; Logue et al., 2016), prior photochemical degradation (this study; Reader & Miller, 2014), and other factors. In general, however, we found that microbial degradation consistently resulted in a small increase in humic-like CDOM fluorescence, and this increase is enhanced after exposure to light. Overall, microbial degradation offsets the loss of humic-like CDOM fluorescence by photobleaching. Furthermore, microbial degradation within the estuary is an autochthonous source of humic-like fluorescence typically associated with DOM of terrigenous origin. Ultimately, the change in CDOM optical properties down-estuary is the combination of microbial and photochemical degradation of terrigenous inputs, and autochthonous inputs of CDOM that are also subject to microbial and photochemical processing.

Jug Bay is the most human-influenced site in terms of nutrient inputs and is also dominated by different (mostly non-persistent emergent) vegetation and soil characteristics than the other sites; as a result, it had both extremely photoreactive and bioavailable CDOM compared to the other marshes. The microbially mediated loss of humic-like fluorescing CDOM at Jug Bay resulted in a smaller offset of photobleaching loss; therefore, this would likely result in lower concentrations of aromatic and high molecular weight CDOM

persisting in the estuary. Because the protein-like CDOM fluorescence at Jug Bay is also photoreactive, this would also likely decrease with UV-exposure down-estuary. This has implications for how nutrient loading and eutrophic conditions in marsh-estuary systems might influence estuarine optical properties and biogeochemical cycling; a shift to more eutrophic marsh systems associated with more photo- and bio-labile CDOM could lead to higher rates of CDOM degradation and DOC loss in estuaries and, therefore, fewer inputs of refractory CDOM down-estuary and, ultimately, to marine environments. However, future work examining down-estuary trends seasonally across marshes of differing characteristics (e.g., eutrophic vs. oligotrophic marsh-systems, marshes with differing vegetation) is needed.

In summary, our study has shown that CDOM source and UV exposure history play an important role in CDOM transformation processes, which vary seasonally, between marsh-systems, and down-estuary. We have shown that the 0.2 μm fraction should not be assumed to be sterile, since enough inoculum passes through the filter to result in significant microbial growth; this stresses the need for other methods of microbial growth inhibition that do not interfere with CDOM optics or photoreactivity in order to isolate the impacts of photobleaching alone. Few studies have examined the quality, bioavailability and photoreactivity of CDOM exported from marshes, and even fewer have compared marshes with varying characteristics and across seasons. Our study illustrates the role of photodegradation on bioavailability, and how these two processes interplay in marsh-estuarine systems to transform, degrade, and produce CDOM of differing qualities down-estuary. This would be particularly useful for comparison to biogeochemical model outputs to further constrain rates and fluxes in estuarine systems (J. B. Clark et al., 2020, 2019). Our results also have applications to remote sensing, which, in tandem with in situ measurements, can improve estimates of CDOM photoreactivity and bioavailability in coastal environments based on the characteristics of both the terrestrial and aquatic coastal landscape, such as land-use, marsh vegetation or soil, and in-water phytoplankton and sediment concentrations; this can be applied to help quantify carbon fluxes at scales much larger than a single marsh or sub-estuarine system.

Data Availability Statement

The data used in this study are available in an online repository (http://doi.org/10.5281/zenodo.4542308).

Acknowledgments
This work was supported by the National Aeronautics and Space Administration (NASA) grant NNX14AP06G and the National Science Foundation (NSF) grant DEB-1556556, with additional support from NASA grant NNX14AM37G and NOAA Earth System Sciences and Remote Sensing Technologies award NA16SEC4810008. The authors would like to thank Dr. P. Megonigal, A. Peresta, and J. Mendez for their support during the field and laboratory measurements.

References

Aulló-Maestro, M. E., Hunter, P., Spyrakos, E., Mercatoris, P., Kovács, A., Horváth, H., et al. (2016). Spatio-seasonal variability of chromophoric dissolved organic matter absorption and responses to photobleaching in a large shallow temperate lake. *Biogeosciences*, *14*, 1215–1233. https://doi.org/10.5194/bg-14-1215-2017

Bianchi, T. S., Osburn, C., Shields, M. R., Yvon-Lewis, S., Young, J., Guo, L., & Zhou, Z. (2014). Deepwater horizon oil in Gulf of Mexico waters after 2 years: Transformation into the dissolved organic matter pool. *Environmental Science and Technology*, *48*(16), 9288–9297. https://doi.org/10.1021/es501547b

Brailsford, F. L., Glanville, H. C., Marshall, M. R., Golyshin, P. N., Johnes, P. J., Yates, C. A., et al. (2017). Microbial use of low molecular weight DOM in filtered and unfiltered freshwater: Role of ultra-small microorganisms and implications for water quality monitoring. *The Science of the Total Environment*, *598*, 377–384. https://doi.org/10.1016/j.scitotenv.2017.04.049

Bricaud, A., Morel, A., & Prieur, L. (1981). Absorption by dissolved organic matter of the sea (yellow substance) in the UV and visible domains1. *Limnology & Oceanography*, *26*(1), 43–53. https://doi.org/10.4319/lo.1981.26.1.0043

Chen, M., & Jaffé, R. (2014). Photo- and bio-reactivity patterns of dissolved organic matter from biomass and soil leachates and surface waters in a subtropical wetland. *Water Research*, *61*, 181–190. https://doi.org/10.1016/j.watres.2014.03.075

Clark, C. D., Litz, L. P., & Grant, S. B. (2008). Saltmarshes as a source of chromophoric dissolved organic matter (CDOM) to Southern California coastal waters. *Limnology & Oceanography*, *53*(5), 1923–1933. https://doi.org/10.4319/lo.2008.53.5.1923

Clark, J. B., Long, W., & Hood, R. R. (2020). A comprehensive estuarine dissolved organic carbon budget using an enhanced biogeochemical model. *Journal of Geophysical Research: Biogeosciences*, *125*(5), 1–21. https://doi.org/10.1029/2019jg005442

Clark, J. B., Neale, P. J., Tzortziou, M., Cao, F., & Hood, R. R. (2019). A mechanistic model of photochemical transformation and degradation of colored dissolved organic matter. *Marine Chemistry*, *214*. https://doi.org/10.1016/j.marchem.2019.103666

Coble, P. G. (1996). Characterization of marine and terrestrial DOM in seawater using excitation-emission matrix spectroscopy. *Marine Chemistry*, *51*, 325–346. https://doi.org/10.1016/0304-4203(95)00062-3

Cory, R. M., Harrold, K. H., Neilson, B. T., & Kling, G. W. (2015). Controls on dissolved organic matter (DOM) degradation in a headwater stream: The influence of photochemical and hydrological conditions in determining light-limitation or substrate-limitation of photo-degradation. *Biogeosciences*, *12*, 6669–6685. https://doi.org/10.5194/bg-12-6669-2015

Dai, M., Yin, Z., Meng, F., Liu, Q., & Cai, W.-J. (2012). Spatial distribution of riverine DOC inputs to the ocean: An updated global synthesis. *Current Opinion in Environmental Sustainability*, *4*, 170–178. https://doi.org/10.1016/j.cosust.2012.03.003

Dalzell, B. J., Minor, E. C., & Mopper, K. M. (2009). Photodegradation of estuarine dissolved organic matter: A multi-method assessment of DOM transformation. *Organic Geochemistry*, *40*, 243–257. https://doi.org/10.1016/j.orggeochem.2008.10.003

Elhadidy, A. M., van Dyke, M. I., Peldszus, S., & Huck, P. M. (2016). Application of flow cytometry to monitor assimilable organic carbon (AOC) and microbial community changes in water. *Journal of Microbiological Methods*, *130*, 154–163. https://doi.org/10.1016/j.mimet.2016.09.009

Fellman, J. B., Amore, D. V. D., Hood, E., & Boone, R. D. (2008). Fluorescence characteristics and biodegradability of dissolved organic matter in forest and wetland soils from coastal temperate watersheds in southeast Alaska. *Biogeochemistry*, *88*(2), 169–184. https://doi.org/10.1007/s10533-008-9203-x

Fellman, J. B., Hood, E., & Spencer, R. G. M. (2010). Fluorescence spectroscopy opens new windows into dissolved organic matter dynamics in freshwater ecosystems: A review. *Limnology & Oceanography*, *55*(6), 2452–2462. https://doi.org/10.4319/lo.2010.55.6.2452

Fellman, J. B., Petrone, K. C., & Grierson, P. F. (2011). Source, biogeochemical cycling, and fluorescence characteristics of dissolved organic matter in an agro-urban estuary. *Limnology & Oceanography*, *56*(1), 243–256. https://doi.org/10.4319/lo.2011.56.1.0243

Guo, W., Xu, J., Wang, J., Wen, Y., Zhuo, J., & Yan, Y. (2010). Characterization of dissolved organic matter in urban sewage using excitation emission matrix fluorescence spectroscopy and parallel factor analysis. *Journal of Environmental Sciences*, *22*(11), 1728–1734. https://doi.org/10.1016/s1001-0742(09)60312-0

Hansell, D., Carlson, C., Repeta, D., & Schlitzer, R. (2009). Dissolved organic matter in the ocean: A controversy stimulates new insights. *Oceanography*, *22*, 202–211. https://doi.org/10.5670/oceanog.2009.109

Hedges, J. I. (1992). Global biogeochemical cycles: Progress and problems. *Marine Chemistry*, *39*, 67–93. https://doi.org/10.1016/0304-4203(92)90096-s

Helms, J. R., Stubbins, A., Ritchie, J. D., Minor, E. C., Kieber, D. J., & Mopper, K. (2008). Absorption spectral slopes and slope ratios as indicators of molecular weight, source, and photobleaching of chromophoric dissolved organic matter. *Limnology & Oceanography*, *53*(3), 955–969. https://doi.org/10.4319/lo.2008.53.3.0955

Hernes, P. J. (2003). Photochemical and microbial degradation of dissolved lignin phenols: Implications for the fate of terrigenous dissolved organic matter in marine environments. *Journal of Geophysical Research*, *108*(C9), 3291. https://doi.org/10.1029/2002jc001421

Jordan, T., Correll, D., Miklas, J., & Weller, D. (1991). Long-term trends in estuarine nutrients and chlorophyll, and short-term effects of variation in watershed discharge. *Marine Ecology Progress Series*, *75*(2–3), 121–132. https://doi.org/10.3354/meps075121

Jordan, T. E., Correll, D. L., Miklas, J., & Weller, D. E. (1991). Nutrients and chlorophyll at the interface of a watershed and an estuary. *Limnology & Oceanography*, *36*(2), 251–267. https://doi.org/10.4319/lo.1991.36.2.0251

Jordan, T. E., Correll, D. L., & Whigham, D. F. (1983). Nutrient flux in the Rhode river: Tidal exchange of nutrients by brackish marshes. *Estuarine, Coastal and Shelf Science*, *17*, 651–667. https://doi.org/10.1016/0272-7714(83)90032-x

Kahle, D., & Wickham, H. (2013). ggmap: Spatial Visualization with ggplot2. *The R Journal*, *5*(1), 144–161. https://doi.org/10.32614/rj-2013-014

Karrh, R., Domotor, D., Golden, R., Karrh, L., Landry, B., Romano, W., et al. (2013). *Patuxent river water quality and habitat assessment*. Maryland Department of Natural Resources.

Kirchman, D., Dittel, A., Findlay, S., & Fischer, D. (2004). Changes in bacterial activity and community structure in response to dissolved organic matter in the Hudson River, New York. *Aquatic Microbial Ecology*, *35*, 243–257. https://doi.org/10.3354/ame035243

Kothawala, D. N., Murphy, K. R., Stedmon, C. A., Weyhenmeyer, G. A., & Tranvik, L. J. (2013). Inner filter correction of dissolved organic matter fluorescence. *Limnology and Oceanography: Methods*, *11*, 616–630. https://doi.org/10.4319/lom.2013.11.616

Lee, S., Kang, Y.-C., & Fuhrman, J. (1995). Imperfect retention of natural bacterioplankton cells by glass fiber filters. *Marine Ecology Progress Series*, *119*, 285–290. https://doi.org/10.3354/meps119285

Liu, J., Li, B., Wang, Y., Zhang, G., Jiang, X., & Li, X. (2019). Passage and community changes of filterable bacteria during microfiltration of a surface water supply. *Environment International*, *131*, 104998 . https://doi.org/10.1016/j.envint.2019.104998

Logue, J. B., Stedmon, C. A., Kellerman, A. M., Nielsen, N. J., Andersson, A. F., Laudon, H., et al. (2016). Experimental insights into the importance of aquatic bacterial community composition to the degradation of dissolved organic matter. *The ISME Journal*, *10*, 533–545. https://doi.org/10.1038/ismej.2015.131

Lønborg, C., Davidson, K., Álvarez-Salgado, X. A., & Miller, A. E. J. (2009). Bioavailability and bacterial degradation rates of dissolved organic matter in a temperate coastal area during an annual cycle. *Marine Chemistry*, *113*, 219–226. https://doi.org/10.1016/j.marchem.2009.02.003

Lu, Y., Bauer, J. E., Canuel, E. A., Yamashita, Y., Chambers, R. M., & Jaffé, R. (2013). Photochemical and microbial alteration of dissolved organic matter in temperate headwater streams associated with different land use. *Journal of Geophysical Research: Biogeoscience*, *118*, 566–580. https://doi.org/10.1002/jgrg.20048

Luef, B., Frischkorn, K. R., Wrighton, K. C., Holman, H. Y. N., Birarda, G., Thomas, B. C., et al. (2015). Diverse uncultivated ultra-small bacterial cells in groundwater. *Nature Communications*, *6*, 1–8. https://doi.org/10.1038/ncomms7372

MacDonell, M. T., & Hood, M. A. (1982). Isolation and characterization of ultramicrobacteria from a gulf coast estuary. *Applied and Environmental Microbiology*, *43*(3), 566–571. https://doi.org/10.1128/aem.43.3.566-571.198

Maie, N., Scully, N. M., Pisani, O., & Jaffé, R. (2007). Composition of a protein-like fluorophore of dissolved organic matter in coastal wetland and estuarine ecosystems. *Water Research*, *41*, 563–570. https://doi.org/10.1016/j.watres.2006.11.006

Medeiros, P. M., Seidel, M., Gifford, S. M., Ballantyne, F., Dittmar, T., Whitman, W. B., & Moran, M. A. (2017). Microbially-mediated transformations of estuarine dissolved organic matter. *Frontiers in Marine Science*, *4*, 69. https://doi.org/10.3389/fmars.2017.00069

Meybeck, M. (1982). Carbon, nitrogen, and phosphorus transport by world rivers. *American Journal of Science*, *282*, 401–450. https://doi.org/10.2475/ajs.282.4.401

Miller, W. L., & Moran, M. A. (1997). Interaction of photochemical and microbial processes in the degradation of refractory dissolved organic matter from a coastal marine environment. *Limnology & Oceanography*, *42*, 1317–1324. https://doi.org/10.4319/lo.1997.42.6.1317

Moran, M. A., Sheldon, W. M., & Sheldon, J. E. (1999). Biodegradation of riverine dissolved organic carbon in five estuaries of the southeastern United States. *Estuaries*, *22*(1), 55–64. https://doi.org/10.2307/1352927

Moran, M. A., Sheldon, W. M., Jr, & Zepp, R. G. (2000). Carbon loss and optical property changes during long-term photochemical and biological degradation of estuarine dissolved organic matter. *Limnology & Oceanography*, *45*(6), 1254–1264. https://doi.org/10.4319/lo.2000.45.6.1254

Murphy, K. R., Hambly, A., Singh, S., Henderson, R. K., Baker, A., Stuetz, R., & Khan, S. J. (2011). Organic matter fluorescence in municipal water recycling schemes: Toward a unified PARAFAC model. *Environmental Science and Technology*, *45*(7), 2909–2916. https://doi.org/10.1021/es103015e

Murphy, K. R., Stedmon, C. A., Wenig, P., & Bro, R. (2014). OpenFluor- an online spectral library of auto-fluorescence by organic compounds in the environment. *Analytical Methods*, *6*(3), 658–661. https://doi.org/10.1039/c3ay41935e

Neale, P. J., & Fritz, J. J. (2002). Experimental exposure of plankton suspensions to polychromatic ultraviolet radiation for determination of spectral weighting functions. *Ultraviolet Ground- and Space-Based Measurements, Models, and Effects*, *4482*, 291–296. https://doi.org/10.1117/12.452930

Nelson, N. B., Carlson, C. A., & Steinberg, D. K. (2004). Production of chromophoric dissolved organic matter by Sargasso Sea microbes. *Marine Chemistry*, *89*, 273–287. https://doi.org/10.1016/j.marchem.2004.02.017

Nixon, S. W. (1980). Between coastal marshes and coastal waters—a review of twenty years of speculation and research on the role of salt marshes in estuarine productivity and water chemistry. In P. Hamilton, & K. B. Macdonald (Eds.), *Estuarine and wetland processes* (pp. 438–525). Plenum Press. https://doi.org/10.1007/978-1-4757-5177-2_20

Obayashi, Y., & Suzuki, S. (2019). High growth potential of transiently 0.2-μm-filterable bacteria with extracellular protease activity in coastal seawater. *Plankton Benthos Research*, *14*(4), 276–286. https://doi.org/10.3800/pbr.14.276

Osburn, C. L., Boyd, T. J., Montgomery, M. T., Bianchi, T. S., Coffin, R. B., & Paerl, H. W. (2016). Optical proxies for terrestrial dissolved organic matter in estuaries and coastal waters. *Frontiers in Marine Science*, *2*, 127. https://doi.org/10.3389/fmars.2015.00127

Osburn, C. L., Handsel, L. T., Mikan, M. P., Paerl, H. W., & Montgomery, M. T. (2012). Fluorescence tracking of dissolved and particulate organic matter quality in a river-dominated estuary. *Environmental Science and Technology*, *46*(16), 8628–8636. https://doi.org/10.1021/es3007723

Osburn, C. L., Handsel, L. T., Peierls, B. L., & Paerl, H. W. (2016). Predicting sources of dissolved organic nitrogen to an estuary from an agro-urban coastal watershed. *Environmental Science and Technology*, *50*(16), 8473–8484. https://doi.org/10.1021/acs.est.6b00053

Osburn, C. L., Mikan, M. P., Etheridge, J. R., Burchell, M. R., & Birgand, F. (2015). Seasonal variation in the quality of dissolved and particulate organic matter exchanged between a salt marsh and its adjacent estuary. *Journal of Geophysical Research: Biogeosci.*, *120*, 1430–1449. https://doi.org/10.1002/2014jg002897

Osburn, C. L., & Stedmon, C. A. (2011). Linking the chemical and optical properties of dissolved organic matter in the Baltic-North Sea transition zone to differentiate three allochthonous inputs. *Marine Chemistry*, *126*(1–4), 281–294. https://doi.org/10.1016/j.marchem.2011.06.007

Osburn, C. L., Zagarese, H. E., Morris, D. P., Hargreaves, B. R., & Cravero, W. E. (2001). Calculation of spectral weighting functions for the solar photobleaching of chromophoric dissolved organic matter in temperate lakes. *Limnology & Oceanography*, *46*(6), 1455–1467. https://doi.org/10.4319/lo.2001.46.6.1455

Perry, J. E., & Atkinson, R. B. (1997). Plant diversity along a salinity gradient of four marshes on the York and Pamunkey rivers in Virginia. *Castanea*, *62*(2), 112–118.

Pinsonneault, A. J., Megonigal, J. P., Neale, P. J., Tzortziou, M., Canuel, E. A., Pondell, C. R., et al. (2020). Dissolved organic carbon sorption dynamics in tidal marsh soils. *Limnology and Oceanography*, *66*(1), 214–225.

Putter, A. (1907). Der Stoffhaushalt des Meeres. *Allgemeine Physiologie*, *7*, 321–368.

Qualls, R. G., Haines, B. L., & Swank, W. T. (1991). Fluxes of dissolved organic nutrients and humic substances in a deciduous forest. *Ecology*, *72*(1), 254–266. https://doi.org/10.2307/1938919

Reader, H. E., & Miller, W. L. (2014). The efficiency and spectral photon dose dependence of photochemically induced changes to the bioavailability of dissolved organic carbon. *Limnology & Oceanography*, *59*(1), 182–194. https://doi.org/10.4319/lo.2014.59.1.0182

Retelletti Brogi, S., Derrien, M., & Hur, J. (2019). In-depth assessment of the effect of sodium azide on the optical properties of dissolved organic matter. *Journal of Fluorescence*, *29*(4), 877–885. https://doi.org/10.1007/s10895-019-02398-w

Rochelle-Newall, E. J., & Fisher, T. R. (2002). Production of chromophoric dissolved organic matter fluorescence in marine and estuarine environments: An investigation into the role of phytoplankton. *Marine Chemistry*, *77*, 7–21. https://doi.org/10.1016/s0304-4203(01)00072-x

Rose, K. C., Neale, P. J., Tzortziou, M., Gallegos, C. L., & Jordan, T. E. (2018). Patterns of spectral, spatial, and long-term variability in light attenuation in an optically complex sub-estuary. *Limnology & Oceanography*, *64*, 257–272. https://doi.org/10.1002/lno.11005

Santos, L., Santos, E. B. H., Dias, J. M., Cunha, A., & Almeida, A. (2014). Photochemical and microbial alterations of DOM spectroscopic properties in the estuarine system Ria de Aveiro. *Photochemical and Photobiological Sciences*, *13*, 1146–1159. https://doi.org/10.1039/c4pp00005f

Schlesinger, W. H., & Bernhardt, E. S. (2013). *Biogeochemistry: An analysis of global change* (3rd ed.). Elsevier, Inc.

Seitzinger, S. P., Harrison, J. A., & Dumont, E. (2005). Sources and delivery of carbon, nitrogen, and phosphorus to the coastal zone: An overview of global nutrient export from watersheds (NEWS) models and their application. *Global Biogeochemical Cycles*, *19*, 1–11. https://doi.org/10.1029/2005gb002606

Shultz, M., Pellerin, B., Aiken, G., Martin, J., & Raymond, P. (2018). High frequency data exposes nonlinear seasonal controls on dissolved organic matter in a large watershed. *Environmental Science and Technology*, *52*, 5644–5652. https://doi.org/10.1021/acs.est.7b04579

Stedmon, C. A., & Bro, R. (2008). Characterizing dissolved organic matter fluorescence with parallel factor analysis: A tutorial. *Limnology and Oceanography: Methods*, *6*, 572–579. https://doi.org/10.4319/lom.2008.6.572b

Stedmon, C. A., & Markager, S. (2005). Tracing the production and degradation of autochthonous fractions of dissolved organic matter by fluorescence analysis. *Limnology & Oceanography*, *50*(5), 1415–1426. https://doi.org/10.4319/lo.2005.50.5.1415

Swarth, C. W., Delgado, P., & Whigham, D. F. (2013). Vegetation dynamics in a tidal freshwater wetland: A long-term study at differing scales. *Estuaries and Coasts*, *36*, 559–574. https://doi.org/10.1007/s12237-012-9568-x

Tanaka, K., Kuma, K., Hamasaki, K., & Yamashita, Y. (2014). Accumulation of humic-like fluorescent dissolved organic matter in the Japan Sea. *Scientific Reports*, *4*, 1–7. https://doi.org/10.1038/srep05292

Thurman, E. M. (1985). *Organic geochemistry of natural waters*. Martinus Nijhoff/Dr W. Junk Publishers.

Tranvik, L. J. (1988). Availability of dissolved organic carbon for planktonic bacteria in oligotrophic lakes of differing humic content. *Microbial Ecology*, *16*, 311–322. https://doi.org/10.1007/bf02011702

Tranvik, L. J. (1993). Microbial transformation of labile dissolved organic matter into humic-like matter in seawater. *FEMS Microbiology Ecology*, *12*, 177–183. https://doi.org/10.1111/j.1574-6941.1993.tb00030.x

Tranvik, L. J., Olofsson, H., & Bertilsson, S. (1999). Photochemical effects on bacterial degradation of dissolved organic matter in lake water. In *Microbial Biosystems: New Frontiers, Proceedings of the 8th International Symposium on Microbial Ecology* (pp. 193-200). Atlantic Canada Society for Microbial Ecology Halifax.

Tzortziou, M., Neale, P., Megonigal, J., Pow, C., & Butterworth, M. (2011). Spatial gradients in dissolved carbon due to tidal marsh outwelling into a Chesapeake Bay estuary. *Marine Ecology Progress Series*, *426*, 41–56. https://doi.org/10.3354/meps09017

Tzortziou, M., Neale, P. J., Osburn, C. L., Megonigal, J. P., Maie, N., & JaffÉ, R. (2008). Tidal marshes as a source of optically and chemically distinctive colored dissolved organic matter in the Chesapeake Bay. *Limnology & Oceanography*, *53*(1), 148–159. https://doi.org/10.4319/lo.2008.53.1.0148

Tzortziou, M., Osburn, C. L., & Neale, P. J. (2007). Photobleaching of dissolved organic material from a tidal marsh-estuarine system of the Chesapeake Bay†. *Photochemistry and Photobiology*, *83*, 782–792. https://doi.org/10.1111/j.1751-1097.2007.00142.x

Volk, C. J., Volk, C. B., & Kaplan, L. A. (1997). Chemical composition of biodegradable dissolved organic matter in streamwater. *Limnology & Oceanography*, *42*(1), 39–44. https://doi.org/10.4319/lo.1997.42.1.0039

Wagner, S., Jaffé, R., Cawley, K., Dittmar, T., & Stubbins, A. (2015). Associations between the molecular and optical properties of dissolved organic matter in the Florida everglades, a model coastal wetland system. *Frontiers in Chemistry*, *3*, 66. https://doi.org/10.3389/fchem.2015.00066

Wang, Y., Hammes, F., Boon, N., & Egli, T. (2007). Quantification of the filterability of freshwater bacteria through 0.45, 0.22, and 0.1 μm pore size filters and shape-dependent enrichment of filterable bacterial communities. *Environmental Science and Technology*, *41*(20), 7080–7086. https://doi.org/10.1021/es0707198

Wang, Y., Hammes, F., Düggelin, M., & Egli, T. (2008). Influence of size, shape, and flexibility on bacterial passage through micropore membrane filters. *Environmental Science and Technology*, *42*(17), 6749–6754. https://doi.org/10.1021/es800720n

Ward, N. D., Megonigal, J. P., Bond-Lamberty, B., Bailey, V. L., Butman, D., Canuel, E. A., et al. (2020). Representing the function and sensitivity of coastal interfaces in Earth system models. *Nature Communications*, *11*(1), 1–14. https://doi.org/10.1038/s41467-020-16236-2

Wetzel, R. G. (1992). Gradient-dominated ecosystems: Sources and regulatory functions of dissolved organic matter in freshwater ecosystems. *Hydrobiologia*, *229*, 181–198. https://doi.org/10.1007/bf00007000

Windham-Myers, L., Cai, W.-J., Alin, S. R., Andersson, A., Crosswell, J., Herrmann, J. M., et al. (2018). Chapter 15: Tidal wetlands and estuaries. In N. Cavallaro, G. Shrestha, R. Birdsey, M. A. Mayes, R. G. Najjar, S. C. Reed, et al. (Eds.), *Second state of the carbon cycle report (SOCCR2): A sustained assessment report*. U.S. Global Change Research Program. Retrieved from https://doi.org/10.7930/SOCCR2.2018.Ch15

Yamashita, Y., Jaffé, R., Maie, N., & Tanoue, E. (2008). Assessing the dynamics of dissolved organic matter (DOM) in coastal environments by excitation emission matrix fluorescence and parallel factor analysis (EEM-PARAFAC). *Limnology & Oceanography*, *53*(5), 1900–1908. https://doi.org/10.4319/lo.2008.53.5.1900

Yamashita, Y., Scinto, L. J., Maie, N., & Jaffé, R. (2010). Dissolved organic matter characteristics across a subtropical wetland's landscape: Application of optical properties in the assessment of environmental dynamics. *Ecosystems*, *13*, 1006–1019. https://doi.org/10.1007/s10021-010-9370-1

Zhang, Y., Liu, X., Osburn, C. L., Wang, M., Qin, B., & Zhou, Y. (2013). Photobleaching response of different sources of chromophoric dissolved organic matter exposed to natural solar radiation using absorption and excitation-emission matrix spectra. *PLoS ONE*, *8*(10), e77515. https://doi.org/10.1371/journal.pone.0077515

References From the Supporting Information

DuPont (2011). *DuPont fluoropolymers*. http://eyecular.com/wp-content/uploads/2017/05/7.-DuPont-2011-Tefzel-Fluoropolymer-Properties-Handbook.pdf

Fritz, J., Neale, P., Davis, R., & Peloquin, J. (2008). Response of Antarctic phytoplankton to solar UVR exposure: Inhibition and recovery of photosynthesis in coastal and pelagic assemblages. *Marine Ecology Progress Series*, *365*, 1–16. https://doi.org/10.3354/meps07610

Henry, B. J., Carlin, J. P., Hammerschmidt, J. A., Buck, R. C., Buxton, L. W., Fiedler, H., et al. (2018). A critical review of the application of polymer of low concern and regulatory criteria to fluoropolymers. *Integrated Environmental Assessment and Management*, *14*(3), 316–334. https://doi.org/10.1002/ieam.4035

Ruggaber, A., Dlugi, R., & Nakajima, T. (1994). Modelling radiation quantities and photolysis frequencies in the troposphere. *Journal of Atmospheric Chemistry*, *18*, 171–210. https://doi.org/10.1007/bf00696813